ANTIOXIDANTS & REDOX SIGNALING
Volume 18, Number 2, 2013

DOI: 10.1089/ars.2011.4491

Therapeutics

ORIGINAL RESEARCH COMMUNICATION

Targeting Nrf2-Mediated Gene Transcription by Extremely Potent Synthetic Triterpenoids Attenuate Dopaminergic Neurotoxicity in the MPTP Mouse Model of Parkinson's Disease

Navneet Ammal Kaidery,[1] Rebecca Banerjee,[2] Lichuan Yang,[2] Natalya A. Smirnova,[3] Dmitry M. Hushpulian,[4] Karen T. Liby,[5] Charlotte R. Williams,[5] Masayuki Yamamoto,[6] Thomas W. Kensler,[7] Rajiv R. Ratan,[3] Michael B. Sporn,[5] M. Flint Beal,[2] Irina G. Gazaryan,[3] and Bobby Thomas[1]

Abstract

Although the etiology of Parkinson's disease (PD) remains unclear, ample empirical evidence suggests that oxidative stress is a major player in the development of PD and in 1-methyl-4-phenyl-1,2,3,6-tetrahydropyridine (MPTP) neurotoxicity. Nuclear factor E2-related factor 2 (Nrf2) is a redox-sensitive transcription factor that upregulates a battery of antioxidant response element (ARE)-driven antioxidative and cytoprotective genes that defend against oxidative stress. ***Aims:*** We evaluated whether the strategy of activation of Nrf2 and its downstream network of cytoprotective genes with small molecule synthetic triterpenoids (TP) attenuate MPTP-induced PD in mice. ***Results:*** We show that synthetic TP are thus far the most potent and direct activators of the Nrf2 pathway using a novel Neh2-luciferase reporter. They upregulate several cytoprotective genes, including those involved in glutathione biosynthesis *in vitro*. Oral administration of TP that were structurally modified to penetrate the brain-induced messenger RNA and protein levels for a battery of Nrf2-dependent cytoprotective genes reduced MPTP-induced oxidative stress and inflammation, and ameliorated dopaminergic neurotoxicity in mice. The neuroprotective effect of these TP against MPTP neurotoxicity was dependent on Nrf2, since treatment with TP in Nrf2 knockout mice failed to block against MPTP neurotoxicity and induce Nrf2-dependent cytoprotective genes. ***Innovation:*** Extremely potent synthetic TP that are direct activators of the Nrf2 pathway block dopaminergic neurodegeneration in the MPTP mouse model of PD. ***Conclusion:*** Our results indicate that activation of Nrf2/antioxidant response element (ARE) signaling by synthetic TP is directly associated with their neuroprotective effects against MPTP neurotoxicity and suggest that targeting the Nrf2/ARE pathway is a promising approach for therapeutic intervention in PD. *Antioxid. Redox Signal.* 18, 139–157.

Introduction

Parkinson's disease (PD) is a progressive neurodegenerative movement disorder characterized by a profound loss of midbrain dopamine (DA) neurons in the substantia nigra pars compacta (SNpc). Despite intensive research, the etiology of PD still remains elusive, and current treatments are inadequate to slow or stop the degenerative process (32). Oxidative damage has been proposed to play a major role in aging and neurodegenerative disorders such as PD (17). Although causal relationships between oxidative damage and PD remain to be defined fully, evidence to date has shown that oxidative stress can be toxic to midbrain dopaminergic neurons. The indices of oxidative damage to these neurons are increased much earlier than actual neuronal loss, and are therefore suggested to serve as a triggering event in the development of PD (7, 24). Bolstering the capacity of a cell to cope with oxidants may be a useful strategy to prevent the onset and/or to delay the progression of PD.

[1]Departments of Pharmacology & Toxicology and Neurology, Georgia Health Sciences University, Augusta, Georgia.
[2]Department of Neurology and Neuroscience, Weill Medical College of Cornell University, New York, New York.
[3]Department of Neurology and Neuroscience, Burke Medical Research Institute, White Plains, New York.
[4]Department of Enzymology, School of Chemistry, Moscow State University, Moscow, Russia.
[5]Department of Pharmacology, Dartmouth Medical School, Hanover, New Hampshire.
[6]Department of Medicinal Biochemistry, Tohoku University, Aoba-ku, Sendai, Japan.
[7]Department of Pharmacology and Chemical Biology, University of Pittsburgh, Pittsburgh, Pennsylvania.

Innovation

Despite years of evidence for the involvement of oxidative stress in Parkinson's disease (PD), no effective antioxidant treatment has proven effective in the clinic. Using a novel reporter, we demonstrate that synthetic triterpenoids (TP) that were structurally modified to penetrate the blood–brain barrier are the most potent and direct activators of the redox-sensitive transcription factor nuclear factor E2-related factor 2 (Nrf2) in upregulating a battery of antioxidant response element (ARE)-driven antioxidative and cytoprotective genes both *in vitro* and *in vivo*. Oral administration of these TP blocked dopaminergic neurotoxicity in mice induced by the parkinsonian neurotoxin 1-methyl-4-phenyl-1,2,3,6-tetrahydropyridine (MPTP), by activating the Nrf2/ARE pathway in an Nrf2-dependent fashion, suggesting that targeting Nrf2-mediated gene transcription is a promising approach for therapeutic intervention in PD.

One means of increasing the antioxidant potential of a cell is through the nuclear Cap-n-Collar basic region leucine zipper transcription factor nuclear factor E2-related factor 2 (Nrf2) (21). Nrf2 functions as a critical mediator of an adaptive response to counteract oxidative stress. Under basal conditions, Nrf2 is tethered to its cytosolic inhibitor Kelch-like ECH-associated protein 1 (Keap1), which facilitates its ubiquitination and proteolytic degradation. In the presence of electrophiles or under oxidative conditions, Nrf2 escapes degradation and translocates to the nucleus, where it binds the antioxidant response elements (AREs), a consensus gene sequence present in the promoter region of a large number of genes encoding cytoprotective proteins (37).

There is increasing evidence that Nrf2/ARE signaling is impaired in PD. The capacity to induce an Nrf2-mediated cytoprotective response declines with age, which is the main risk factor for PD (37). In postmortem brains from PD patients, Nrf2 is localized in the nucleus, and the expression of ARE-driven genes such as NADPH quinone oxidoreductase 1 (*Nqo1*) and hemeoxygenase 1 (*Ho-1*) is increased (30, 33, 51), suggesting a neuroprotective response to block oxidative stress (43). Moreover, genetic studies have identified a functional haplotype in the *Nrf2* gene promoter, which confers high transcriptional activity and a protective response, in two groups of European PD patients (46). Studies in animals demonstrate that Nrf2-deficient mice are hypersensitive to PD-causing toxins, whereas Nrf2 overexpression either by genetic means or through pharmacological activation renders a neuroprotective response (3, 4, 16, 42). These findings suggest that targeting the Nrf2 pathway could have important clinical benefits for the treatment of PD.

Synthetic triterpenoids (TP) such as 2-cyano-3-,12-dioxooleana-1,9 (11)-dien-28-oic acid (CDDO) and its derivatives are potent activators of the Nrf2/ARE pathway (8, 22, 23, 49). Many of these synthetic TP cross the blood–brain barrier (BBB) and are pharmacodynamically active in the brain (48, 49), but improved brain levels can be achieved with new structural analogs such as the ethylamide (TP-319) and trifluoroethylamide (TP-500) of CDDO (10, 36). Here, we compared the previously studied synthetic TP (TP-224) (48) with its two newer structural analogs (TP-319 and TP-500) modified to improve BBB permeability, and studied their abilities to activate the Nrf2/ARE signaling both *in vitro* and *in vivo* and attenuate experimental Parkinsonism in mice. Our current study is substantially innovative from the previous work (48), because (i) we used a novel Neh2-luc reporter assay for the first time to demonstrate that all three synthetic TP are equipotent and direct activators of the Nrf2 pathway (by disrupting the Nrf2-Keap1 binding) and more potent than the canonical Nrf2 activators (tert-butylhydroquinone [TBHQ] and sulforaphane); (ii) we performed docking experiments using a computer model for the intervening region (IVR) of Keap1 and showed the TP C1 potent alkylation site right against Cys226 and predicted that a cysteine residue that may be forced to form a disulfide bridge with Cys226 is Cys298 on Keap, and that all analogs of TP fit similarly into this site; and lastly, (iii) the addition of ethylamide (TP-319) and trifluoroethylamide (TP-500) groups to the parent TP molecule significantly increased BBB permeability, resulting in increased potency in activating the Nrf2 pathway and rendering neuroprotective effects against 1-methyl-4-phenyl-1,2,3,6-tetrahydropyridine (MPTP) neurotoxicity in an Nrf2-dependent manner at nanomolar concentrations compared to TP-224. These results suggest that selective targeting of the Nrf2/ARE pathway by extremely potent, BBB-permeable synthetic TP serves as a credible strategy for therapeutic intervention in PD.

Results

Synthetic TP are the most potent and direct activators of the Nrf2 pathway identified by the Neh2-luc reporter

Synthetic TP containing an activated cyanoenone Michael acceptor motif are extremely potent alkylating agents and are known to activate Nrf2-signaling pathway in a low nanomolar range (8). TP-224, TP-319, and TP-500 have similar structure, except for the substitutions at the C17 carboxygroup aimed at improving BBB permeability (Fig. 1A, Supplementary Fig. S1; Supplementary Data are available online at www.liebertpub.com/ars). To analyze the effect of substitutions, we tested all three TP in a Neh2-luc *in vitro* reporter assay. The P_{cmv}-driven Neh2-luc reporter supports the constitutive, intracellular synthesis of a novel fusion protein composed of the Neh2 domain of Nrf2 and firefly luciferase and is a perfect tool to monitor the direct effect of a particular compound on the first step controlling Nrf2 stability, that is, Nrf2-Keap1 and/or Keap1-Cul3 interaction (35). Comparison of TP-224, TP-319, and TP-500 TP shows that all compounds are potent activators of Nrf2, indistinguishable within an experimental error, and working in the nanomolar range, whereas classical Nrf2 activators like TBHQ and sulforaphane work in the micromolar range (Fig. 1B). The absence of TP effect on the hypoxia-inducible factor (HIF) ODD-luc reporter assay in the studied concentration range confirms the specificity of their action on the Neh2-luc reporter (Supplementary Fig. S2A). The substitutions in TP-319 and TP-500 aimed at improving BBB permeability (27) in comparison with the previously used TP-224 (48) did not compromise the original potency of TP as Nrf2 activators as judged by the *in vitro* cell-based reporter assay.

The advantage of the Neh2-luc assay is its immediate response and superior sensitivity, which permits direct monitoring of reporter activation kinetics within minutes of drug administration (35). The timecourse of reporter activation shows a distinct lag-period shortening with rising concentrations of TP-224 (and exactly the same for TP-319 and

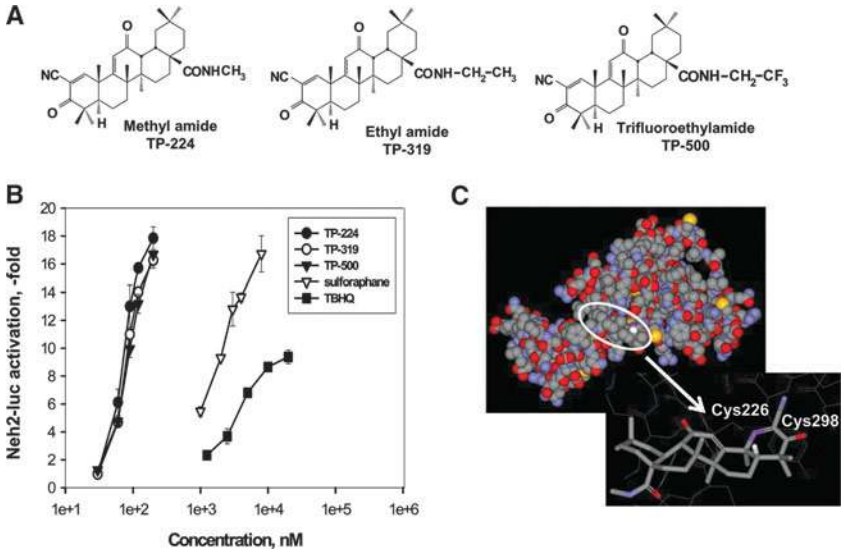

FIG. 1. Synthetic TP are extremely potent activators of Nrf2/ARE signaling. (A) Chemical structure of synthetic TP, CDDO-methylamide (TP-224), CDDO-ethylamide (TP-319), and CDDO-trifluoroethylamide (TP-500). **(B)** Comparison of the three TP in Neh2-luc reporter activation with common Nrf2 activators sulforaphane and TBHQ in semi-logarithmic coordinates (1e+3=1 μM). **(C)** Docking of TP-224 into the model structure of Keap1 intervening domain (IVR): C1 of TP-224, the site of alkylation (shown in *purple*), is oriented toward Cys226, while carbonyl at C3 toward Cys298. Modeling and docking procedures as described in Methods. ARE, antioxidant response element; CDDO, 2-cyano-3-,12-dioxooleana-1,9 (11)-dien-28-oic acid; IVR, intervening region; Keap1, Kelch-like ECH-associated protein 1; Nrf2, nuclear factor E2-related factor 2; TBHQ, tert-butylhydroquinone; TP, triterpenoids.

TP-500) that has been observed for other alkylating agents such as auranofin, but not andrographolide (Supplementary Figs. S1 and S2B–D). The subnanomolar potency of synthetic TP observed in *in vitro* experiments clearly points to the specific character of their alkylation of Keap1. The majority of Keap1 cysteines are localized in the IVR of Keap1, except for Cys151. No crystal structure of IVR is available; however, its model has been built and used for virtual screening purposes: 2 potent hits identified and confirmed (47). We reproduced their model using the same protein as a template for modeling, and performed docking of the triterpenoid TP-224. The best docking result is shown in Figure 1C, with triterpenoid C1 potential alkylation site right against Cys226. The latter has been identified among alkylation sites for TBHQ using ultrahigh-performance liquid chromatography–tandem mass spectrometry analysis (1), as well as for electrophilic nitrofatty acids (19), and in addition, has been proposed to form an intramolecular disulfide with Cys613 from the Kelch domain upon oxidation with hydrogen peroxide and nitrosative agents (12). In our model, a cysteine residue that may be forced to form a disulfide bridge with Cys226 is Cys298, which in its reduced form in the IVR model coordinates triterpenoid's C3 carbonyl oxygen. A bulky substitution at the C17 position in the triterpenoid will interfere with docking. The actual site of TP-224 interaction with Keap1 still has to be determined because of the speculative character of the IVR model; however, there is no doubt that there has to be a specific site for TP-224 binding to Keap1.

Synthetic TP activate the Nrf2 pathway in vitro

We previously showed that structural modification of oleanolic acid derivatives, specifically the CDDO class of synthetic TP, can activate Nrf2/ARE signaling both *in vitro* and *in vivo* (8, 10, 22, 36, 48, 49). In this study, we tested the relative potency of synthetic TP (TP-224, TP-319 and TP-500) in comparison to the classical Nrf2 activator TBHQ to induce the Nrf2 pathway in N27 rat dopaminergic cells. Immunoblot analyses show that treatment of TP (at doses 50, 100, and 200 n*M*) and TBHQ (at doses 5, 10, and 20 μM) dose-dependently upregulated protein levels for Nrf2 and its downstream target HO-1 in N27 cells at 4 h (Supplementary Fig. S3A, B). Significantly, TP (at nanomolar concentrations) were more potent in inducing the Nrf2 pathway than TBHQ (only effective at a micromolar range). Among the TP, TP-319 and TP-500 were more potent in activating the Nrf2 pathway than TP-224 in N27 cells (Supplementary Fig. S3) and in human neuroblastoma SHSY5Y cells (data not shown). We previously reported activation of Nrf2 and its downstream target genes by TP-224 in SHSY5Y cells (48); in the present study, we focused on the structural analogs TP-319 and TP-500 (Fig. 1A).

We tested the ability of TP-319 and TP-500 to induce nuclear translocation of Nrf2. Human neuroblastoma SHSY5Y cells were treated with 100 n*M* TP-319 or TP-500, and the control groups were treated with dimethylsulfoxide (DMSO) and processed for subcellular fractionation. As shown by immunoblot analysis, nuclear Nrf2 was significantly increased compared to DMSO-treated cytosolic and nuclear fractions after treatment with TP-319 or TP-500 for 1 and 2 h. The purity of cytosolic and nuclear fractions was confirmed by probing these preparations with anti-aldolase and anti-poly ADP ribose polymerase 1 (PARP1), respectively (Fig. 2A). We observed that both TP-319 and TP-500 administration resulted in abundant Nrf2 accumulation in nuclear fractions, and its migration was slightly higher than its actual molecular weight, a feature that we failed to observe with our prior

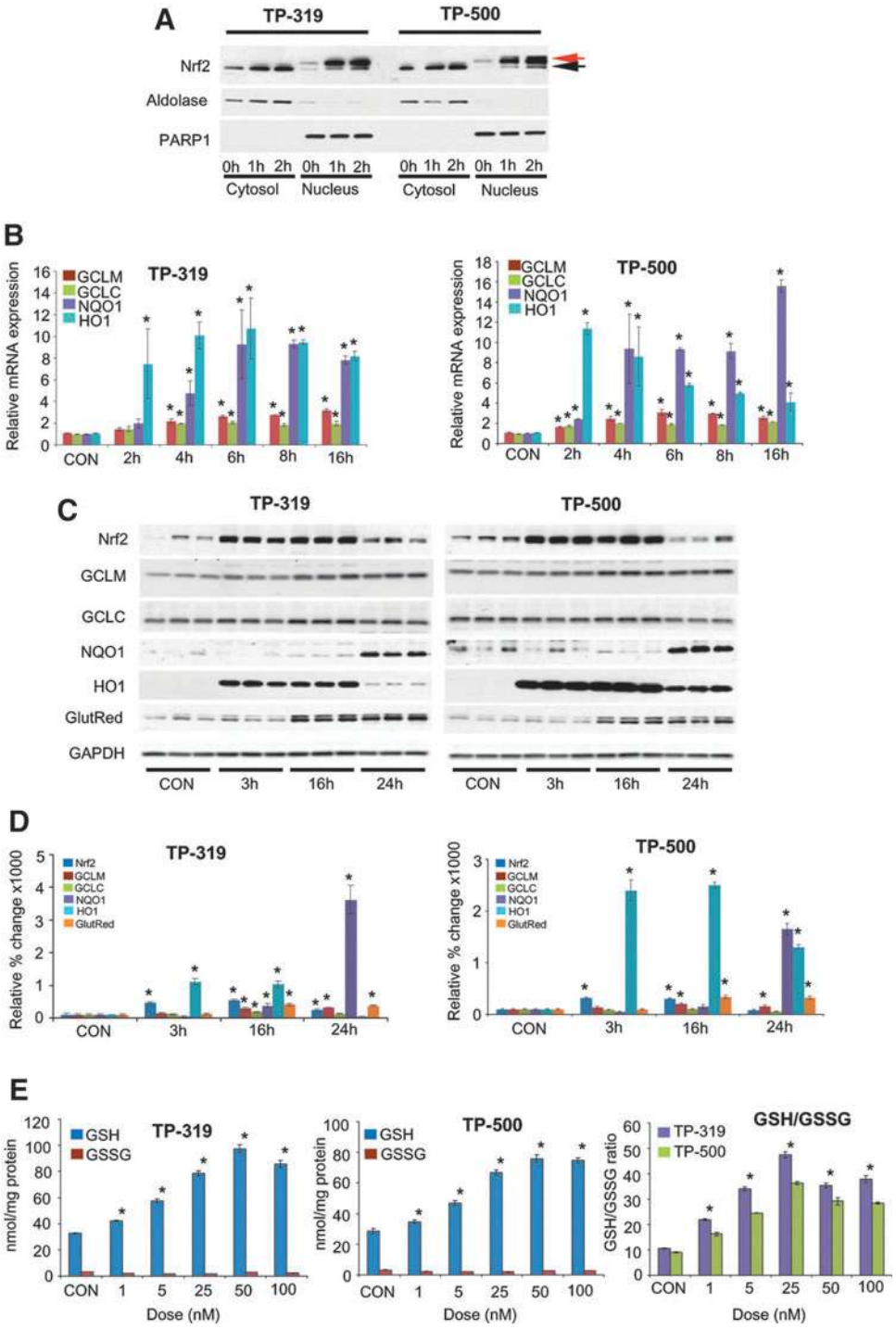

FIG. 2. Synthetic TP activate Nrf2/ARE signaling *in vitro*. **(A)** Nuclear translocation of Nrf2 from cytosol after treatment with TP-319 and TP-500. Triterpenoid treatment leads to a shift in Nrf2 migration, which is the major species in the nucleus (*red arrow*) compared to the cytosolic Nrf2 (*black arrow*). Aldolase and PARP1 are used as markers for cytosolic and nuclear fractions, respectively. **(B)** Quantitative RT-PCR analysis showing relative mRNA levels of ARE genes after TP-319 and TP-500 administration. Bars represent mean ± SEM. $*p < 0.05$ compared to controls, ($n = 5$/time point). **(C)** Western blot analysis and **(D)** densitometry analysis of ARE proteins and relative change of ARE proteins after TP-319 and TP-500 treatment ($n = 3$/time point). Bars represent mean ± SEM. $*p < 0.05$ compared to controls. **(E)** Intracellular GSH, GSSG and the ratio (GSH/GSSG) at 24 h following TP-319 and TP-500 treatment. Bars represent mean ± SEM. $*p < 0.05$ compared to controls, ($n = 4$/time point). GlutRed, *Gsr* (glutathione reductase); GSH, reduced glutathione; GSSG, oxidized glutathione; mRNA, messenger RNA; PARP1, poly-ADP ribose polymerase 1; RT-PCR, reverse transcriptase–polymerase chain reaction; SEM, standard error of the mean.

studies with TP-224 (48). Next, we determined whether TP-319- and TP-500-induced nuclear translocation of Nrf2 resulted in significant increases in messenger RNA (mRNA) levels of downstream *ARE* genes. Assessment of mRNA and protein levels for several *ARE* genes in SHSY5Y cells treated with 100 n*M* of TP-319 or TP-500 showed significant upregulation of these *ARE* genes (data not shown). Similarly, N27 cells treated with 100 n*M* of TP-319 and TP-500 resulted in significant increases in mRNA levels of Nrf2-dependent *ARE* genes such as *NQO1*, glutathione cysteine ligase regulatory subunit (*GCLC*), glutathione cysteine ligase modulatory subunit (*GCLM*), and *HO-1* as measured by quantitative reverse transcriptase–polymerase chain reaction (RT-PCR) at 2, 4, 6, 8, and 16 h (Fig. 2B). Consistent with upregulation of mRNA levels for ARE genes, *Nrf2, Gclm, Gclc, Nqo1, Ho-1* and glutathione reductase (*Gsr*) protein levels were also significantly increased at indicated time points as shown by immunoblot (Fig. 2C) and densitometry analysis (Fig. 2D). Since both TP-319 and TP-500 significantly changed levels of genes that regulate glutathione metabolism, we measured cellular levels of reduced (GSH) and oxidized (GSSG) 24 h after treatment with the respective TP. Both TP-319 and TP-500 showed dose-dependent increases in

levels of GSH (Fig. 2E) and corresponding increases in the ratio of GSH/GSSG that saturated at doses higher than 50 nanomoles. Together, our *in vitro* studies suggest that both TP-319 and TP-500 induce nuclear accumulation of Nrf2 to upregulate downstream ARE genes, leading to dose-dependent increases in cellular antioxidants such as GSH.

Synthetic TP activate Nrf2-mediated gene transcription in vivo

Next, we tested the ability of TP-319 and TP-500 to activate Nrf2/ARE signaling *in vivo* in mice. Ten-week-old C57Bl6 mice were given 4 μmol of TP-224, TP-319, and TP-500 twice, 12 h apart by oral gavage. Control animals received vehicle in the same frequency and volume as the triterpenoid drugs. Pharmacokinetic studies showed that in comparison to TP-224, TP-319 and TP-500 when administered at similar doses can achieve significantly higher levels in both the liver (Fig. 3A) and the brain (Fig. 3B) at concentrations that induced activation of the Nrf2 pathway *in vitro* (Figs. 1B and 2). Analysis of mRNA levels of downstream Nrf2-dependent ARE genes by quantitative RT-PCR analysis showed significant (5–25-fold) increases in mRNA levels in the liver for ARE genes such as *GCLM*, *GCLC*, *HO-1*, and *Gsr* at 6 and 9 h after the last dose of TP-319 and TP-500 (Fig. 4A). Striatal mRNA levels of *Nqo1* and *Ho-1* were also significantly upregulated, but genes involved in glutathione biosynthetic machinery such as *Gclm* and *Gclc* and *Gsr* were not upregulated (Fig. 4B). Similarly, in the ventral midbrain, a significant upregulation of mRNA levels of *Nqo1* and *Ho-1* was observed for both TP at 6 and 9 h in addition to significant increases in levels for *Gclm* when treated with TP-319 at 9 h (Fig. 4C). In the cortex, however, only the mRNA levels of *Nqo1* were significantly upregulated at 6 and 9 h, whereas the mRNA levels of other ARE genes were unaffected (Supplementary Fig. S4C). None of the brain regions, including striatum, ventral midbrain, and cortex, showed upregulation of mRNA levels for the ARE genes at 24 and 48 h after the administration of both the TP (Supplementary Fig. S4A, B, D). Consistent with mRNA upregulation in the liver, immunoblot (Fig. 5A) and densitometry analysis (Fig. 5B) showed significant increases in Nrf2

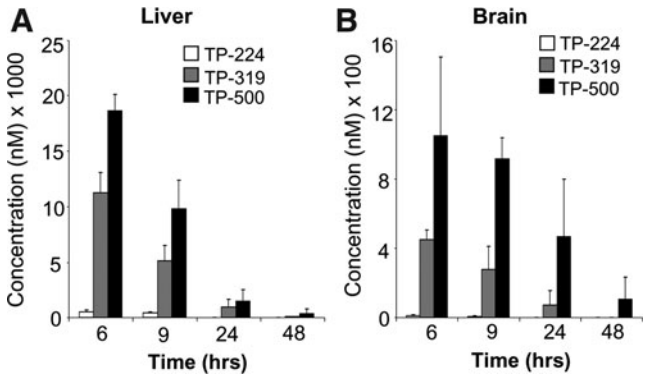

FIG. 3. Relative levels of synthetic TP *in vivo*. (A) Levels of TP-224, TP-319, and TP-500 in the liver and **(B)** brain of C57Bl6 mice after two doses of 4 μmol of respective TP administered 12 h apart by oral gavage and measured at 6, 9, 24, and 48 h after the last dose. Bars represent mean ± SDEV ($n = 4$ mice per group for each time point).

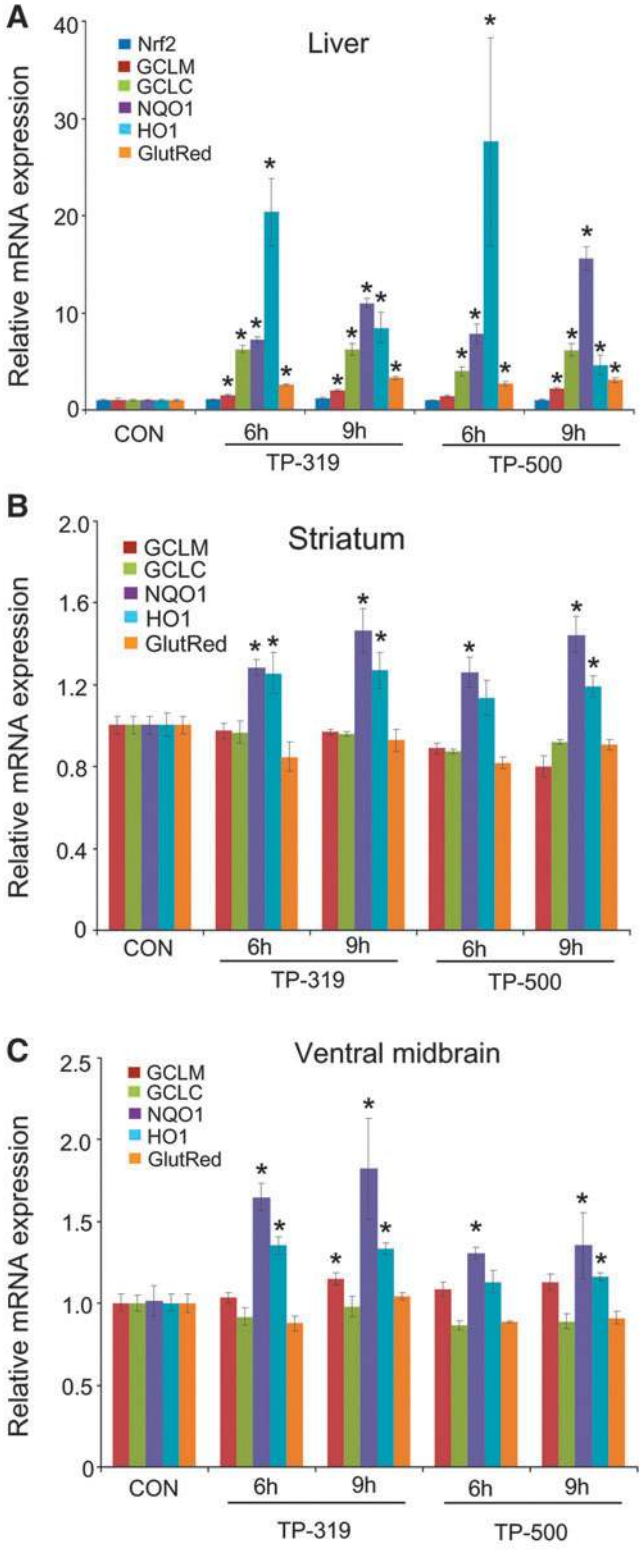

FIG. 4. Synthetic TP upregulate mRNA levels of Nrf2/ARE genes *in vivo*. (A–C) Quantitative RT-PCR analysis showing relative mRNA levels of ARE genes in the liver, striatum, and ventral midbrain after TP-319 and TP-500 treatment. Bars represent mean ± SEM. *$p < 0.05$ compared to controls ($n = 5$/time point).

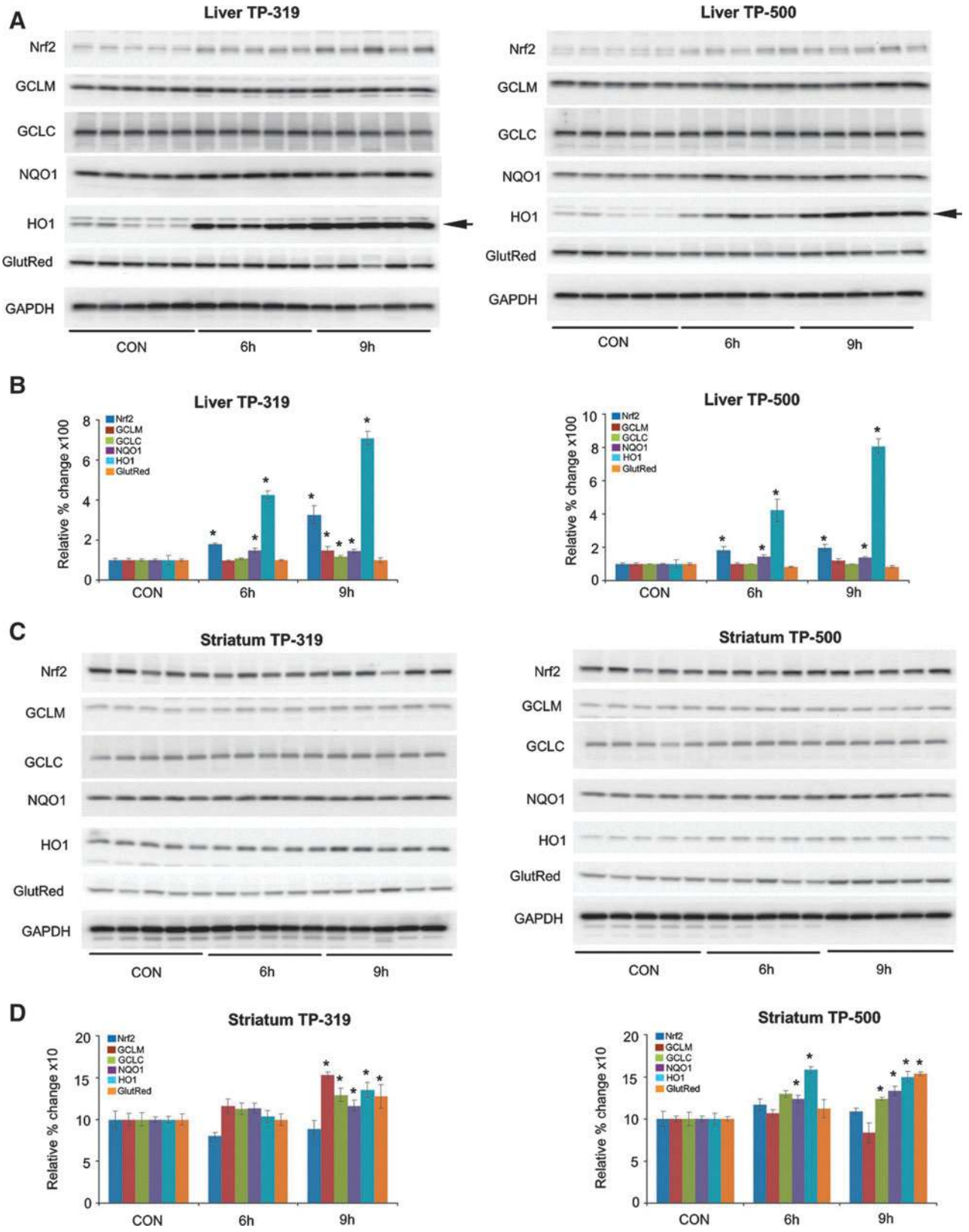

FIG. 5. Synthetic TP upregulate protein levels of Nrf2/ARE genes *in vivo*. Western blot analysis **(A, C)** and densitometry analysis **(B, D)** showing relative change of Nrf2 and downstream ARE proteins in the liver **(A, B)** and striatum **(C, D)** after TP-319 and TP-500 administration. Arrow shows the HO-1 band. Bars represent mean ± SEM. $^*p < 0.05$ compared to controls ($n = 5$/time point). HO-1, hemeoxygenase 1.

and downstream ARE target proteins such as NQO1 and HO-1 at 6 h, whereas Nrf2, NQO1, GCLM, GCLC, and HO-1 were markedly upregulated at 9 h. Immunoblot (Fig. 5C) and densitometry analysis (Fig. 5D) in the striatum confirmed significant increases in GCLM, GCLC, NQO1, HO-1, and Gsr protein levels at 9 h after TP-319 treatment, whereas these protein levels were unaffected at 6 h. In contrast to TP-319, administration of TP-500 resulted in increases in striatal levels of NQO1 and HO-1 by 6 h, whereas GCLC, NQO1, HO-1, and Gsr were markedly upregulated by 9 h without affecting Nrf2 expression. However, in the ventral midbrain, immunoblot (Supplementary Fig. S5A) and densitometry analysis (Supplementary Fig. S5B) showed significant increases only in NQO1 levels 9 h after TP-319 and at 6 and 9 h after TP-500 (Supplementary Fig. S5B). Collectively, these data provide *in vivo* evidence for the ability of both TP-319 and TP-500 to activate the Nrf2-mediated ARE gene transcription that is directly associated with their *in vivo* pharmacokinetic profiles.

Synthetic TP attenuate MPTP neurotoxicity in mice

Several lines of studies suggest that deficiency of Nrf2 in mice leads to increased vulnerability to MPTP neurotoxicity (3, 16, 20), whereas activation of Nrf2-mediated gene transcription either *via* a genetic or pharmacologic approach has shown profound neuroprotective effects against MPTP neurotoxicity (4, 15, 16). Hence, we sought to test if *in vivo* activation of Nrf2/ARE signaling by TP-319 and TP-500 can induce a neuroprotective response against MPTP neurotoxicity. We used an acute paradigm of MPTP administration (10 mg MPTP/kg × 3, every 2 h), known to cause about a 50% loss of striatal DA and its metabolites 3,4-dihydroxyphenylacetic acid (DOPAC) and homovanillic acid (HVA) and a significant loss of tyrosine hydroxylase (TH) immunopositive neurons in the SNpc on the 7th day. Comparison of relative potency of TP in blocking MPTP neurotoxicity found that TP-224, TP-319, and TP-500 dose-dependently (at doses 4, 2, 1, and 0.5 μmol) protected against MPTP-induced loss of striatal DA, DOPAC, and HVA (Table 1). Significantly, TP-319 and TP-500 were more potent in blocking MPTP neurotoxicity than TP-224 at lower doses (0.5 μmol) (Table 1). Consistent with levels of striatal catecholamines, unbiased stereologic counts of total (*i.e.*, Nissl-positive) and TH-positive neurons in SNpc showed a statistically significant loss of neurons in the MPTP group compared to controls. Analysis of total and TH-positive neuronal counts for both TP-319 and TP-500, when administered at either 4 or 0.5 μmol, showed a significant dose-dependent attenuation of MPTP-induced loss of total (*i.e.*, Nissl-positive) and TH-immunopositive neurons as compared to MPTP-treated mice (data not shown). The neuroprotective effects of TP-319 and TP-500 against MPTP-neurotoxicity were not due to impaired metabolism of MPTP to its toxic metabolite 1-methyl-4-phenyl-pyridinium ion (MPP^+). High-performance liquid chromatography (HPLC)–fluorimetric analysis of striatal MPP^+ levels measured 90 min after a single intraperitoneal injection of 30 mg/kg free base MPTP showed no significant difference between the MPTP (12.12 ± 2.09 ng/mg tissue) and TP (TP-319: 11.71 ± 2.5; and TP-500: 12.58 ± 3.79 ng/mg tissue).

To fully characterize the neuroprotective effects of TP-319 and TP-500 in two well-established paradigms of MPTP neurotoxicity, we used an acute (15 mg MPTP/kg × 4, every 2 h) and subacute paradigms of MPTP (30 mg/kg once daily for 5 days) (38). In both the neurotoxic paradigms of MPTP, a dose of 2 μmol of TP-319 and TP-500 was used (see the Methods section for dosing protocol). Neuropathologic evaluations were conducted 1 week after the acute MPTP paradigm and 3 weeks after subacute MPTP. In the acute (Fig. 6A–C) and the subacute (Fig. 6D–F) MPTP paradigms, immunohistochemical analysis for TH-positive neurons in the substantia nigra and striatal dopaminergic nerve terminals (data not shown) demonstrated a marked reduction when compared to saline controls. Both TP-319- and TP-500-treated mice showed significant reductions in the MPTP-induced loss of TH-positive neurons in SNpc (Fig. 6A, D) and striatal dopaminergic nerve terminals (data not shown) when compared to mice treated with MPTP alone. Consistent with TH-immunostaining in SNpc, stereological cell counts of total (*i.e.*, Nissl-positive) and TH-positive neurons showed a statistically significant loss in the MPTP group compared to controls. Both TP-319 and TP-500 administration significantly attenuated the MPTP-induced loss of total and TH-positive neurons compared to MPTP-treated mice (Fig. 6B, E). Consistent with the loss of striatal dopaminergic terminals, HPLC–electrochemical analysis revealed a profound reduction in striatal DA (Fig. 6C, F) and its metabolites (DOPAC and HVA [data not shown]) after MPTP treatment, but both TP-319 and TP-500 significantly rescued against MPTP-induced loss of striatal DA (Fig. 6C, F) and its metabolites (data not shown). Together, these data conclusively prove that both TP-319 and TP-500 not only activate the Nrf2/ARE pathway *in vivo* but also possess great potential in protecting nigrostriatal dopaminergic pathway neurons in the acute and subacute paradigms of MPTP neurotoxicity.

Table 1. Dose–Response Effect of Synthetic Triterpenoids on Acute MPTP-Induced Levels of Striatal Catecholamines

Groups	*Dopamine*	*DOPAC*	*HVA*
Control	101.24 ± 2.04	12.70 ± 0.38	10.20 ± 0.35
MPTP	46.63 ± 3.77[a]	7.43 ± 0.64[a]	7.17 ± 0.30[a]
TP-319 4.0	99.80 ± 3.8	11.9 ± 1.2	9.82 ± 0.6
TP-319 4.0 + MPTP	84.7.2 ± 3.8[b]	11.27 ± 0.52[b]	10.10 ± 0.82[b]
TP-319 2.0 + MPTP	85.98 ± 4.8[b]	12.32 ± 0.68[b]	10.20 ± 0.88[b]
TP-319 1.0 + MPTP	83.98 ± 2.94[b]	12.34 ± 0.54[b]	10.39 ± 0.66[b]
TP-319 0.5 + MPTP	73.77 ± 5.31[b]	11.36 ± 0.82[b]	9.44 ± 0.46[b]
TP-500 4.0	96.4 ± 5.2	11.65 ± 1.4	9.4 ± 1.8
TP-500 4.0 + MPTP	79.60 ± 4.26[b]	9.88 ± 1.8[b]	8.2 ± 0.8[b]
TP-500 2.0 + MPTP	80.38 ± 5.85[b]	10.98 ± 1.1[b]	9.01 ± 0.5[b]
TP-500 1.0 + MPTP	77.40 ± 6.01[b]	12.05 ± 0.89[b]	8.60 ± 0.51[b]
TP-500 0.5 + MPTP	76.26 ± 7.98[b]	11.40 ± 1.06[b]	8.86 ± 0.61[b]
TP-224 4.0	97.88 ± 4.6	11.2 ± 0.9	9.90 ± 1.3
TP-224 4.0 + MPTP	73.46 ± 2.9 [b]	10.20 ± 1.8[b]	8.4 ± 0.42[b]
TP-224 2.0 + MPTP	74.64 ± 3.8 [b]	10.40 ± 1.6[b]	8.7 ± 0.68[b]
TP-224 1.0 + MPTP	71.14 ± 1.77[b]	10.49 ± 1.06[b]	8.49 ± 0.33[b]
TP-224 0.5 + MPTP	65.63 ± 6.85[b]	10.25 ± 0.86[b]	8.34 ± 0.62

Striatal levels of dopamine and its metabolites DOPAC and HVA were measured on the 7th day after MPTP. TP-319, TP-500, and TP-224 were administered at 4, 2, 1, and 0.5 μmol. Data represent mean ± standard error of the mean, [a]$p < 0.001$ compared to control, and [b]$p < 0.001$ compared to the MPTP group ($n = 8$ mice per group).

DOPAC, 3,4-dihydroxyphenylacetic acid; HVA, homovanillic acid; MPTP, 1-methyl-4-phenyl-1,2,3,6-tetrahydropyridine; TP, triterpenoids.

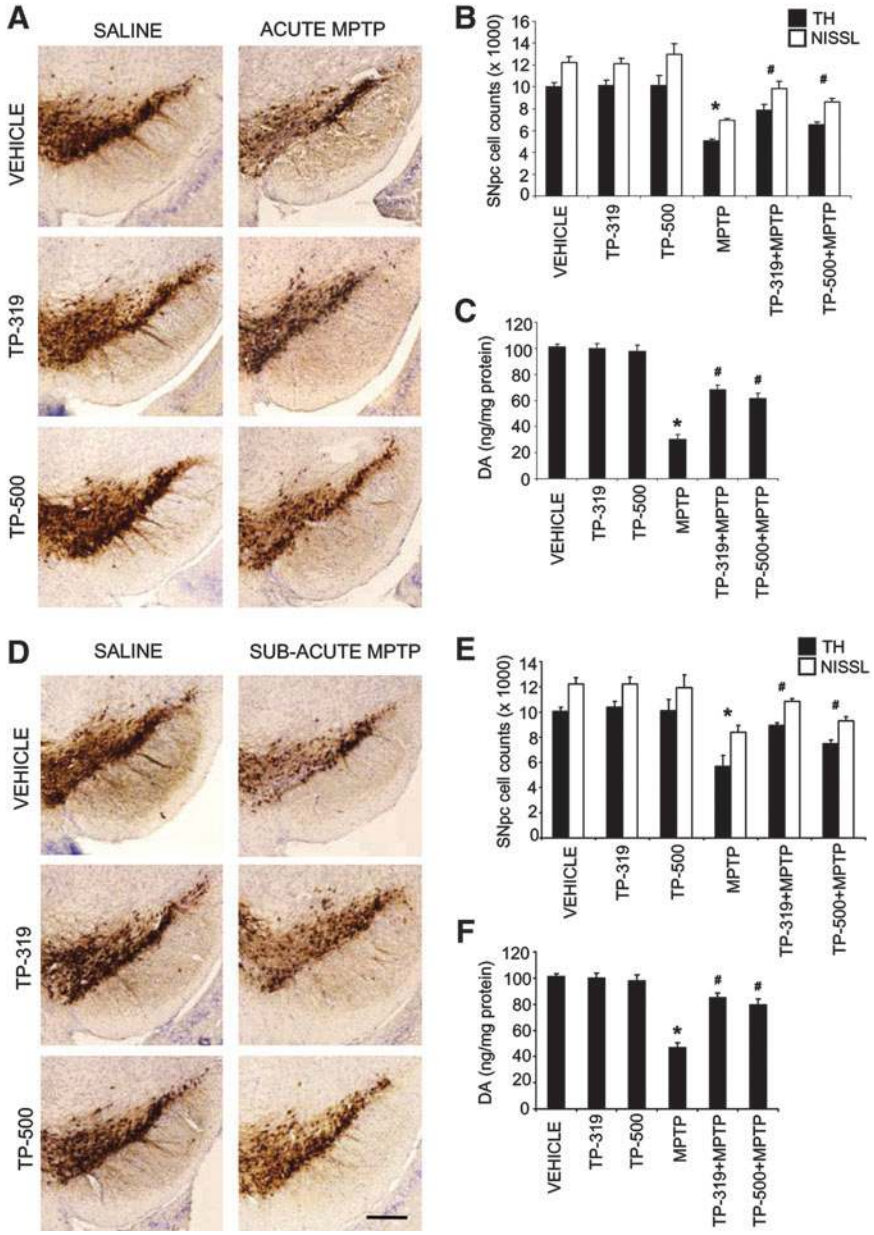

FIG. 6. Neuroprotective effects of synthetic TP in the MPTP model of Parkinson's disease. (A) Immunohistochemical staining for TH and **(B)** stereological analysis of total (NISSL) and TH^+-neurons in the SNpc in the acute MPTP model on the 7th day after treatment with TP-319 and TP-500. Bars represent mean ± SEM. $^*p < 0.05$ compared to saline controls, and $^{\#}p < 0.05$ compared to MPTP ($n = 6$ mice per group). **(C)** Striatal levels of DA measured by HPLC analysis in the acute MPTP model on the 7th day. Bars represent mean ± SEM. $^*p < 0.05$ compared to saline controls, and $^{\#}p < 0.05$ compared to MPTP ($n = 6$ mice per group). **(D)** Immunohistochemical staining for TH and **(E)** in the substantia nigra in the subacute MPTP model on the 21st day after treatment with TP-319 and TP-500. Bas represent mean ± SEM. $^*p < 0.05$ compared to saline controls, and $^{\#}p < 0.05$ compared to MPTP ($n = 6$ mice per group). **(F)** Striatal levels of DA measured by HPLC analysis in the subacute MPTP-model on the 21st day. Bars represent mean ± SEM. $^*p < 0.05$ compared to saline controls, and $^{\#}p < 0.05$ compared to MPTP ($n = 6$ mice per group) (scale bar, 200 μm). DA, dopamine; HPLC, high-performance liquid chromatography; MPTP, 1-methyl-4-phenyl-1,2,3,6-tetrahydropyridine; SNpc, substantia nigra pars compacta; TH, tyrosine hydroxylase.

Synthetic TP block MPTP-induced oxidative stress and inflammation

The MPTP-induced degeneration of nigrostriatal dopaminergic neurons is accompanied by increases in markers of oxidative stress and inflammation in the nigrostriatal pathway. Since Nrf2-mediated gene transcription controls both oxidative stress and inflammation (21, 31), we investigated if the neuroprotective effects of TP-319 and TP-500 are associated with the attenuation of markers of oxidative stress and inflammation. Accordingly, we examined the expression of 3-nitrotyrosine (a marker for protein oxidation produced by reactive nitrogen species) activated CD11b-immunopositive (microglial marker) cells and mRNA levels of the proinflammatory genes, respectively. As shown in Figure 7A, after 48 h of acute MPTP injection (15 mg MPTP/kg × 4, every 2 h), there was a marked increase in accumulation of 3-nitrotyrosine immunoreactivity in the SNpc, which was completely abrogated in mice treated with TP-319 and TP-500. Quantitative analysis of 3-nitrotyrosine immunoreactivity in SNpc showed significantly higher levels after MPTP, which were markedly reduced when mice were treated with TP-319 or TP-500 (Fig. 7B). Administration of TP-319 and TP-500 alone did not affect 3-nitrotyrosine levels in the SNpc and were comparable to controls (data not shown). Similarly, MPTP administration markedly increased markers of inflammation such as reactive microglia at 36 h after acute MPTP administration (15 mg MPTP/kg × 4, every 2 h), whereas in vehicle-treated animals, only a few faintly immunoreactive microglia (Fig. 7C) were observed in the SNpc. Both TP-319 and TP-500 administration resulted in a significant decrease in MPTP-induced microglial activation (Fig. 7C). Consistent with the qualitative changes in CD11b (microglial marker), morphometric

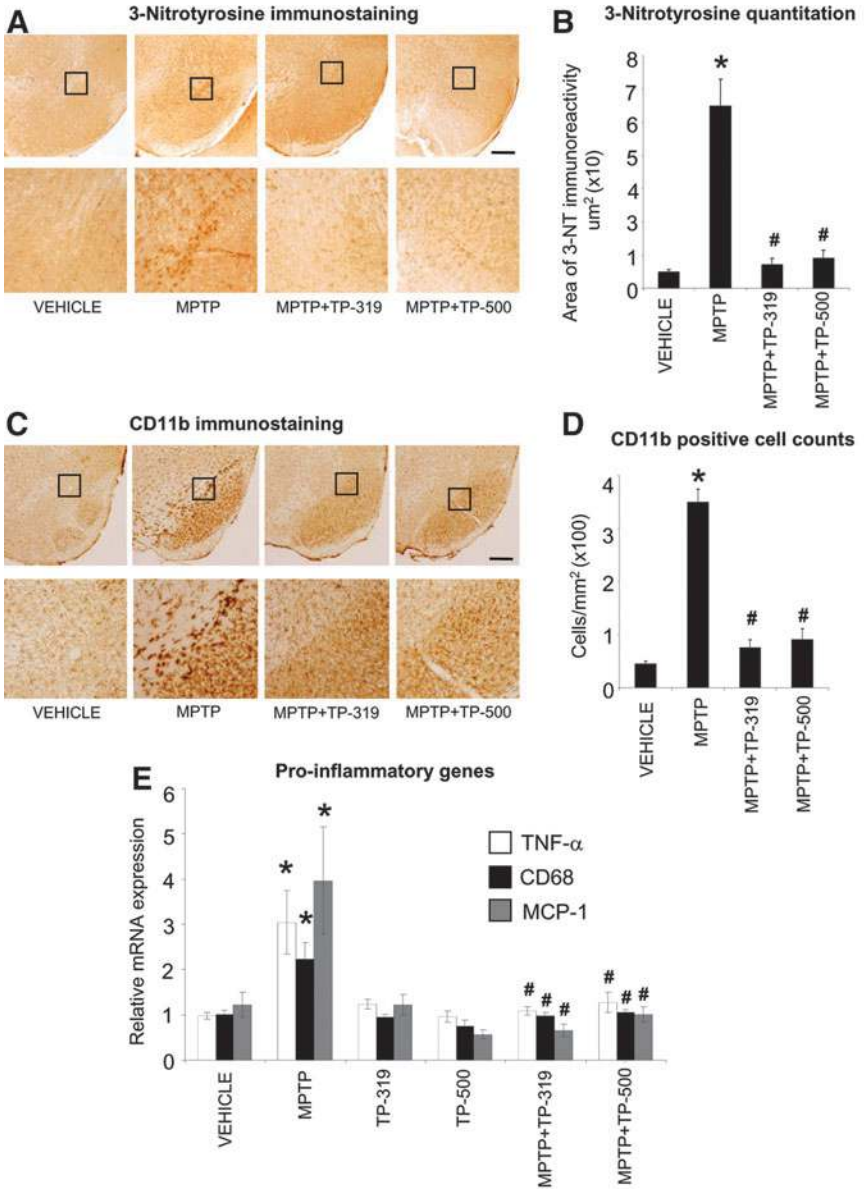

FIG. 7. Synthetic TP attenuate MPTP-induced accumulation of oxidative stress and inflammation. (A) Accumulation of oxidative stress in the substantia nigra demonstrated by 3-nitrotyrosine immunoreactivity 48 h after acute MPTP and following TP-319 and TP-500 treatment; representative images from $n=5$ mice in each group (scale bar, 200 μm). **(B)** Quantitative comparison of area of 3-nitrotyrone immunoreactivity in SNpc 48 h after acute MPTP and following TP-319 and TP-500 treatment. Bars represent mean ± SEM. $^{*}p<0.05$ *versus* saline controls and $^{\#}p<0.05$ *versus* MPTP, ($n=5$). **(C)** CD11b-immunoreactive microglia and **(D)** CD11b-positive microglial cell counts in the substantia nigra 36 h after acute MPTP and treatment with TP-319 and TP-500. Representative images from $n=5$ mice in each group (scale bar, 200 μm). Bars represent mean ± SEM. $^{*}p<0.05$ *versus* saline controls and $^{\#}p<0.05$ *versus* MPTP ($n=5$). **(A)** and **(C)** Area of interest marked by a square is magnified and shown below. **(E)** Levels of proinflammatory genes measured 24 h after last dose of acute MPTP and following TP-319 and TP-500 treatment. Bars represent mean ± SEM. $^{*}p<0.05$ *versus* saline controls and $^{\#}p<0.05$ *versus* MPTP, ($n=5$).

analysis of reactive CD11b-positive microglia showed significantly higher numbers of reactive microglia (Fig. 7D) after MPTP, which were significantly reduced when mice were treated with TP-319 or TP-500 (Fig. 7D). Treatment with TP-319 and TP-500 alone showed similar numbers of activated microglia in the SNpc as in vehicle-treated controls (data not shown). Assessment of the mRNA levels of the proinflammatory cytokine tumor necrosis factor-alpha (Tnf), chemokine [C-C motif] ligand 2 (*Ccl2*, monocyte chemotactic protein 1, *Mcp1*), and microglial activation marker cluster of differentiation 68 (*Cd68*) showed significant increases in the ventral midbrain 24 h after acute MPTP administration (15 mg MPTP/kg × 4, every 2 h) compared to vehicle (Fig. 7E). Both the TP significantly blocked MPTP-induced increases in proinflammatory genes (Fig. 7E). Taken together, these data suggest that the TP-319- and TP-500-induced neuroprotective response against MPTP-neurotoxicity is associated with a marked reduction in markers of oxidative stress and inflammation.

Synthetic TP attenuate MPTP neurotoxicity in an Nrf2-dependent manner

To determine if the neuroprotective effects exerted by TP-319 and TP-500 are indeed *via* the Nrf2-dependent pathway, we evaluated their ability to block MPTP neurotoxicity in wild-type (WT) and Nrf2 knockout (KO) mice. Because Nrf2 KO mice show increased sensitivity to MPTP neurotoxicity as compared to WT mice (3, 4), we delivered a milder dose of MPTP (10 mg MPTP/kg × 4, every 2 h) using an acute intoxication regimen in Nrf2 KO and age-matched WT littermate mice. Both TP-319 and TP-500 were administered at a dose of 2 μmol (see the Methods section for dosing protocol). One week after MPTP administration, immunohistochemical analysis in SNpc demonstrated a marked reduction in TH-immunopositive neurons in WT mice (Fig. 8A) when compared to controls. MPTP administration in Nrf2 KO mice also showed increased vulnerability to the loss of TH-positive neurons as compared to MPTP-treated WT mice. Both TP-319

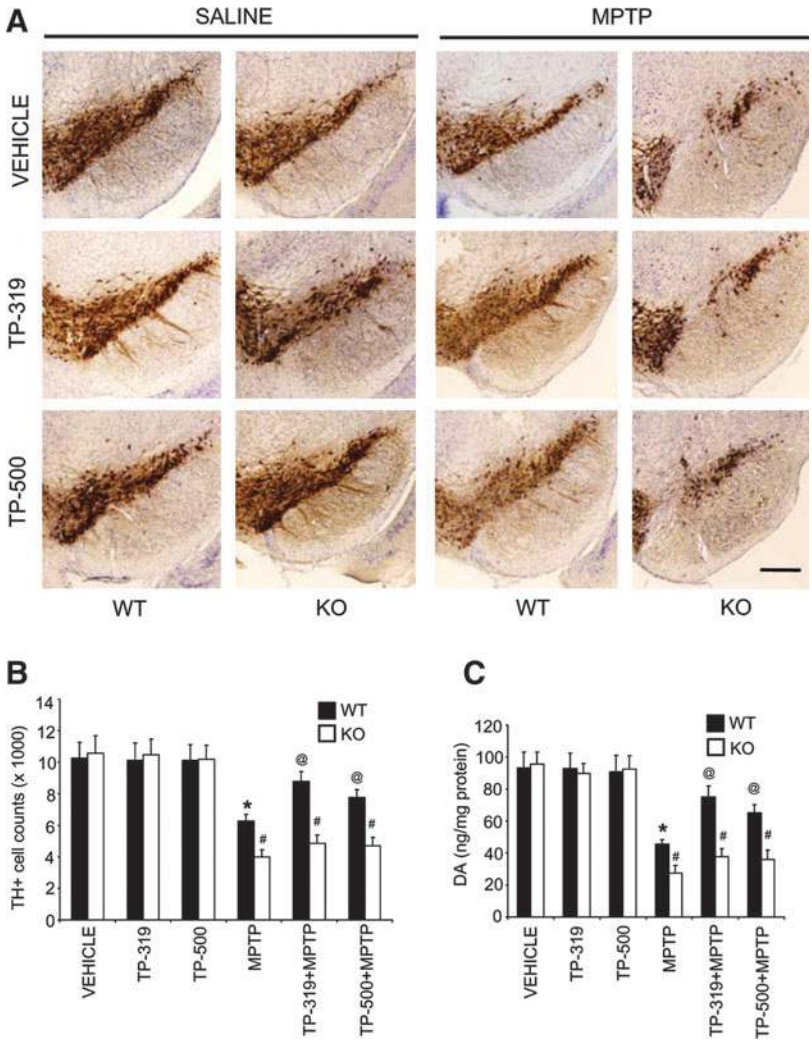

FIG. 8. Selective neuroprotective effects of synthetic TP against MPTP neurotoxicity in WT, but not in Nrf2 KO mice. (A) Immunohistochemical staining for TH in the substantia nigra of WT and Nrf2 KO mice on the 7th day following TP-319 and TP-500 treatment in the acute MPTP model, (scale bar, 200 μm). **(B)** Stereological analysis of total (NISSL) and TH^+-neurons in the SNpc and **(C)** striatal levels of DA measured by HPLC analysis in WT and Nrf2 KO mice. Bars represent mean ± SEM. $^*p < 0.05$ compared to saline controls, and $^{\#}p < 0.05$ compared to WT MPTP ($n = 6$ mice per group), and $^{@}p < 0.05$ compared to WT MPTP. KO, knockout; WT, wild type.

and TP-500 markedly reduced the MPTP-induced loss of TH-positive neurons in the SNpc in WT mice, but failed to protect against MPTP neurotoxicity in Nrf2 KO mice (Fig. 8A). Unbiased stereologic counts of total (*i.e.*, Nissl-positive) (Supplementary Fig. S6A) and TH-immunopositive neurons in SNpc (Fig. 8B) showed a statistically significant loss of neurons in the MPTP group compared to the saline control. Both TP-319 and TP-500 significantly attenuated the MPTP-induced loss of total (Supplementary Fig. S6A) and TH-immunopositive neurons (Fig. 8B) in WT mice, but not in Nrf2 KO mice. HPLC–electrochemical analysis also revealed a profound reduction in striatal DA (Fig. 8C) and its metabolites [DOPAC and HVA (Supplementary Fig. S6B, C)] after MPTP treatment in WT mice compared to saline-injected WT controls. MPTP treatment in Nrf2 KO mice produced a significantly higher depletion of striatal DA (Fig. 8C) and its metabolites [DOPAC and HVA (Supplementary Fig. S6B, C)] as compared to MPTP-treated WT mice. However, both TP-319 and TP-500 treatment rescued the MPTP-induced loss of striatal DA (Fig. 8C) and its metabolites only in the WT mice, but not in Nrf2 KO mice. The lack of neuroprotection in Nrf2 KO mice after synthetic TP against MPTP neurotoxicity was not due to differences in the conversion of MPTP to its toxic metabolite MPP^+, in the Nrf2 KO mice compared to WT mice (Supplementary Table S1). These results demonstrate that the ability of TP-319 and TP-500 to attenuate MPTP neurotoxicity is dependent on the Nrf2 pathway.

Selective activation of Nrf2 mediated gene transcription by synthetic TP in vivo

We evaluated Nrf2-mediated gene transcription in WT and Nrf2 KO mice to determine if the triterpenoid-mediated neuroprotective effects are due to their selective activation of the Nrf2/ARE pathway. Age-matched Nrf2 KO mice and WT littermates, were administered 4 μmol of either TP-319 or TP-500 by oral gavage twice 12 h apart. Control animals of both genotypes received vehicle in the same frequency and volume as the two triterpenoid drugs. As shown by quantitative RT-PCR analysis, mRNA levels of ARE genes such as *Gclm*, *Gclc*, *Ho-1*, and *Gsr* were significantly increased (2–12-fold) in the liver of WT mice at 9 h after the last dose of TP-319 and TP-500 (Fig. 9A). However, this induction of mRNA for target ARE genes was absent in Nrf2 KO mice (Fig. 9A). Immunoblot (Fig. 9B) and corresponding densitometry analysis (Fig. 9C) also showed significant upregulation of protein levels for GCLM, GCLC, and NQO1 in the liver of WT mice after TP-319 and TP-500 treatment. However, basal levels of GCLM, GCLC, and NQO1 protein were significantly lower in vehicle-treated Nrf2 KO mice compared to WT, and administration of either

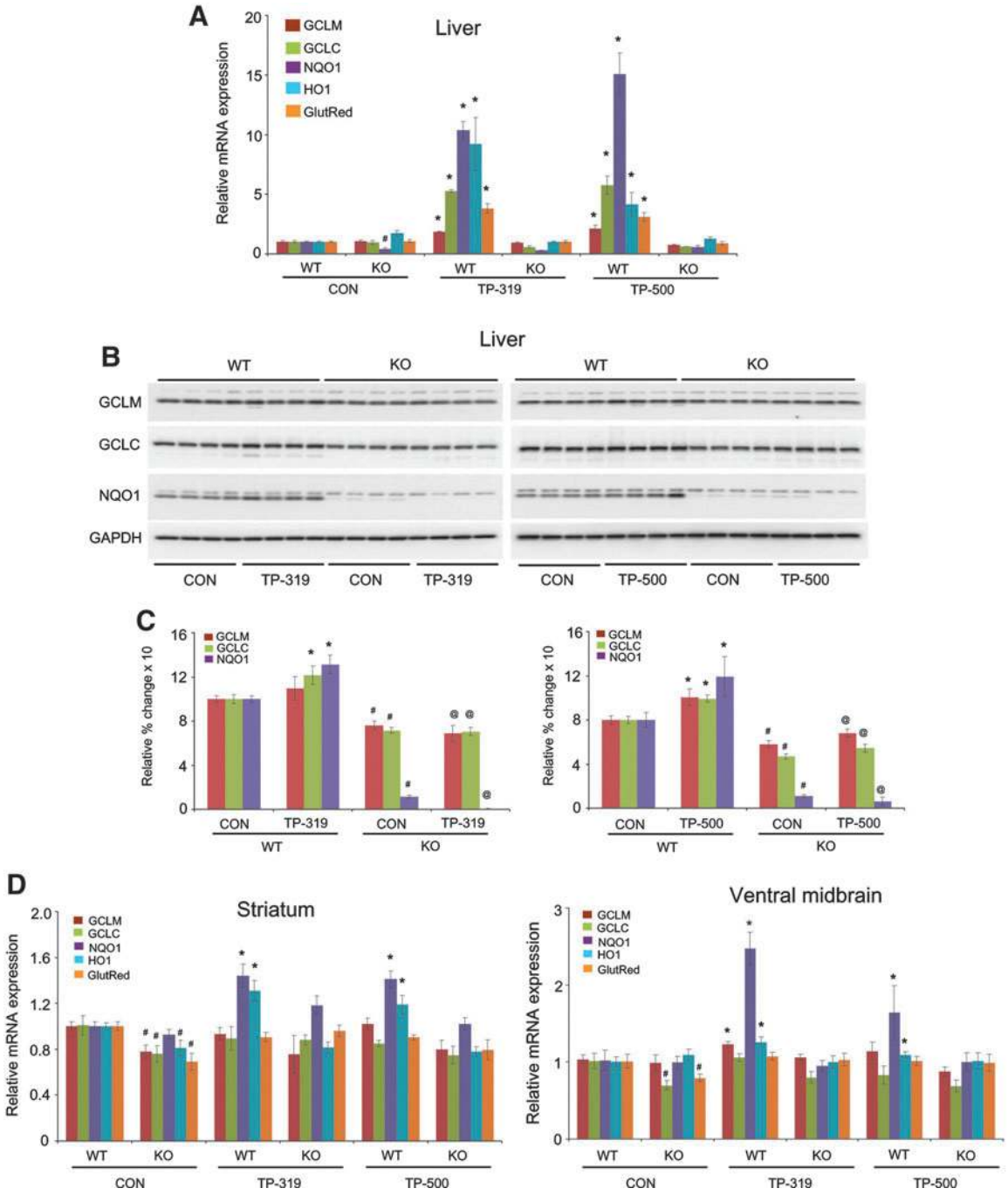

FIG. 9. Selective ARE activation of synthetic TP in WT, but not in Nrf2 KO mice. (A) Quantitative RT-PCR analysis showing relative mRNA levels of ARE genes and **(B)** western blot analysis of ARE proteins in the liver of WT and Nrf2 KO mice 9 h after treatment with TP-319 and TP-500. Bars represent the mean ± SEM. $^{*}p < 0.05$ compared to controls ($n = 5$ mice per group). **(C)** Densitometry analysis of the western blots in **(B)** showing relative change of ARE proteins *, $^{\#}p < 0.05$ compared to WT controls, and $^{@}p < 0.05$ comparing WT TP-319 or TP-500 ($n = 4$). **(D)** Quantitative RT-PCR analysis showing relative mRNA levels of ARE genes in the striatum and ventral midbrain of WT and Nrf2 KO mice after treatment with TP-319 and TP-500. Bars represent the mean ± SEM. $^{*}p < 0.05$ comparing untreated controls, ($n = 5$).

TP-319 or TP-500 failed to upregulate protein levels for any of these genes in the KO mice, suggesting that induction of the ARE pathway is dependent on the presence of a functional Nrf2. In the nigrostriatal system, TP-319 and TP-500 significantly upregulated the mRNA levels of *Nqo1* and *Ho-1* in the striatum of WT mice, whereas Nrf2 KO mice failed to show any induction of mRNA levels for these ARE genes (Fig. 9D). Similarly, TP-319 significantly upregulated *Nqo1* and *Ho-1*, whereas TP-500 significantly increased *Nqo1* in the ventral midbrains of WT mice compared to controls. Both TP-319 and TP-500, however, failed to upregulate ARE genes in the ventral midbrains of Nrf2 KO mice (Fig. 9D). Similar to the liver,

the nigrostriatal system also showed reduced basal gene transcripts for ARE genes *Gclm, Gclc, Ho-1,* and *Gsr* in striatum and *Gclc* and *Gsr* in the ventral midbrains of Nrf2 KO mice (Fig. 9D). Importantly, the differences in induction of Nrf2-mediated downstream ARE activation between WT and Nrf2 KO mice were not due to differences in pharmacokinetic profiles of the triterpenoid drugs in these target organs between the two genotypes (Supplementary Fig. S7). Hence, the observed neuroprotective activity of TP-319 and TP-500 against MPTP neurotoxicity is directly associated with selective activation of Nrf2-mediated gene transcription.

Discussion

The Nrf2 signaling cascade has emerged as a promising pathway for neurotherapeutics by transcriptional modulation of both oxidative stress and inflammation. Current therapies for PD are largely symptomatic and may partially improve the quality of life for patients, but none has been convincingly shown to stop or slow the insidious degenerative process. The pathogenesis of neuronal degeneration in PD is yet to be fully understood; however, oxidative stress appears to be a prominent pathogenic component in PD (17). Based on this, one would postulate that increasing the capacity of dopaminergic neurons to cope with oxidants could serve as an important strategy to prevent the onset and/or to delay the progression of PD. In the past, antioxidants such as vitamin E, vitamin C, *N*-acetylcysteine, and glutathione have been tested in animal models and in clinical trials for several neurodegenerative disorders, including PD (18, 34). However, such approaches that rely predominantly on stoichiometric scavenging of oxidants unfortunately had little or no benefits. An alternative promising therapeutic strategy is to restore redox homeostasis in neurodegenerative disorders by activation of the transcription factor Nrf2, a member of the Cap-n-Collar family of basic leucine-zipper transcription factors that regulates a coordinated adaptive genetic program (26). The ability to selectively induce a battery of cytoprotective and antioxidative enzymes that are directly under the genetic control of a single transcription factor such as Nrf2 may have significant advantages over conventional strategies. One can potentially induce multiple antioxidant pathways and associated neuroprotective responses, which would not be dependent on the antioxidant effects of single or combinations of molecules that are frequently consumed while scavenging toxic-free radical species in a diseased or aging brain. This study identified that synthetic TP such as TP-224, TP-319, and TP-500 are thus far the most potent and direct Nrf2 activators. Among these TP, TP-319 and TP-500 are orally active and extremely potent, with profound neuroprotective properties at nanomolar concentrations in an experimental model of PD by virtue of their ability to activate the Nrf2-signaling cascade.

TP are synthesized by the cyclization of squalene, a triterpene hydrocarbon found ubiquitously in nature (6). Structure–activity analysis shows that α, β-unsaturated carbonyl groups in CDDO at key positions on rings A and C are essential for the striking anti-inflammatory potency, and enable Michael addition with a nucleophilic target (6, 23) similar to Keap 1 (a protein with multiple nucleophilic–SH residues and a cytoplasmic repressor of Nrf2). This reaction activates the phase-2 response, an intrinsic mechanism used by cells to deactivate electrophiles or oxidative stress. We used a novel Neh2-luc reporter and identified that synthetic TP are the most potent and direct activators of the Nrf2 pathway reported to date. The Neh2-luc reporter is extremely sensitive, allowing reporter activation kinetics within minutes of drug administration (35). With increasing concentrations of TP, the reporter activation showed a distinct lag-period shortening similar to alkylating agents such as auranofin, but not andrographolide (Supplementary Figs. S1 and S2B–D). Auranofin is a bulky molecule, known to alkylate active protein thiols (or selenols such as in thioredoxin reductase) by a ligand-exchange mechanism, the so-called sulfhydryl shuttle (29), while andrographolide, a labdane diterpenoid recently patented for the treatment of Amyotrophic Lateral Sclerosis and other neurodegenerative disorders (UK Patent application GB2464813), has an α,β-unsaturated lactone moiety alkylating protein or peptide-active -SH or -NH2 groups by Michael addition followed by dehydration (53). The observed lag-periods for TP may be interpreted as a switch in the rate-limiting step, meaning that there is a step preceding their direct alkylation of Keap1 reactive cysteines. The TP studied are chemically complex molecules, where alkylation should occur at C1 of the ring A [see Fig. 1 in (8) by analogy with the alkylation site in acetylenic tricyclic *bis*(cyanoenone) TBE-1 (9)].

Our computer-modeling experiments using the Keap IVR model found the best docking result with TP C1 as a potent alkylation site against Cys226. The latter has been identified among alkylation sites for TBHQ using mass spectrometry analysis (1), as well as for electrophilic nitrofatty acids (19). The access to this position is much more restricted than to the freely rotating α,β-unsaturated lactone moiety of andrographolide, and thus we may suppose either formation of a specific protein–triterpenoid complex before alkylation actually takes place or a ligand exchange mechanism as in the case of auranofin. The idea of specific interaction between Keap-Nrf2 and TP is supported by the high potency of TP toward the Nrf2-Keap1 system, which is orders of magnitude higher than their potency for targeting the NF-Kb pathway by alkylating critical Cys179 in the active loop of IKK (52). Another interpretation of the observed lags could be membrane permeability or diffusion limitations: of note, the acting concentrations of TP are in the low nanomolar range and at least, one order of magnitude lower than those for andrographolide. The intracellular concentration of the fusion Neh2-luc protein synthesized (recalculated from luciferase activity as 9–10 nM fusion protein formed per hour for 30,000 cell/well density and 233-μ^3 single-cell volume) is comparable with the concentration of TP added. However, the amount of the cell volume is four orders of magnitude less than the incubation medium volume, and thus there is a large excess of alkylating agent. If alkylation is irreversible, the amount of alkylating agent, and not its concentration, is in play, and the observed lag-periods must be ascribed to the mechanistic complexity. Despite the mechanistic details of triterpenoid action on the Keap1-Nrf2-Cul3 complex still await their elucidation, the compounds of this class (bardoloxone) are already in clinical trials (40). Since the alkylating potency of the TP with varied substitutions at the C17 carboxygroup remained unchanged, and the introduced substitutions improved BBB permeability, and new TP are expected to be far more advantageous over TP-224 and result in higher activation of the Nrf2 pathway (Figs. 1 and 3).

We previously reported activation of Nrf2-mediated gene transcription and associated neuroprotective effects of CDDO methyl amide (TP-224) in blocking MPTP-induced PD (48). However, when compared to TP-224, administration of either TP-319 or TP-500 at similar doses produced significantly higher levels of Nrf2 and its downstream ARE target hemeoxygensase 1 in N27 rat dopaminergic cells. These TP when compared to other prototypical Nrf2 activators such as TBHQ and sulforaphane were far more potent in dissociating the Nrf2/Keap1 complex (Fig. 1) or activate ARE-mediated gene transcription both *in vitro* (Supplementary Fig. S3) and *in vivo* (49). Here we found that nanomolar concentrations of both TP-319 and TP-500 in human neuroblastoma SHSY5Y cells and N27 rat dopaminergic cells, activated the Nrf2/ARE pathway, by inducing expression levels of Nrf2 and several downstream antioxidative and cytoprotective genes, including those involved in the glutathione biosynthetic machinery, to subsequently increase GSH levels. Importantly, decrements in the levels of GSH in nigral dopaminergic neurons in incidental Lewy body disease (also known as presymptomatic PD) may play an important role in the development of PD (7). Dose-dependent upregulation of GSH levels at low nanomolar concentrations by TP-319 and TP-500 in dopaminergic cells is consistent with their strong antioxidant actions. Unlike TP-224, both TP-319 and TP-500 were exceptionally potent activators of the Nrf2 pathway, leading to nuclear Nrf2 translocation as early as 1 h. Surprisingly, we found that both TP-319 and TP-500 resulted in Nrf2 migration that was slightly higher than its actual molecular weight, and that was abundant in the nuclear fractions (Fig. 2A) in comparison to the cytosol, or nuclear fractions treated with TP-224 (48). We reasoned this might be a phosphomodification of Nrf2 unique to TP-319 and TP-500 treatment, since it is postulated that phosphorylation of Nrf2 by upstream kinases, especially at serine 40, shuttles cytosolic Nrf2 to the nucleus to activate the Nrf2/ARE pathway (13, 28). Accordingly, we probed our cytosolic and nuclear fractions after triterpenoid treatment with an antiphospho Nrf2 (ser40) antibody. However, we failed to observe increased phosphorylated Nrf2 (ser40) after TP-319 and TP-500 treatment (data not shown). This may also be due to phosphorylation at alternate amino acid residues or other forms of post-translational modifications in Nrf2, yet to be identified. Significantly, the differences in Nrf2 migration patterns due to treatment with different TP were only observed in the liver and N27 rat dopaminergic cells, but not in striatum (Figs. 2C and Fig 5A, C), the reasons of which remain elusive. Despite these differences among various TP, our *in vitro* findings suggest that both TP-319 and TP-500 are equally superior activators of the Nrf2 pathway in comparison to TP-224 and other classical Nrf2 activators like TBHQ and sulforaphane.

In vivo pharmacokinetic studies have shown that the addition of functional groups (ethylamide to TP-319 and trifluoroethylamide to TP-500) enhances brain penetration when compared to the methylamide TP-224, with TP-500 showing the highest penetration in the brain and the longest tissue half-life (Fig. 3) (27, 49). However, despite increased brain availability and the longer half-life for TP-500 compared to TP-319, the ability to induce the Nrf2 signaling in the nigrostriatal pathway or in the cortex of the mice was comparable for both compounds at the doses tested (Figs. 4 and 5). The reasons for these differences are unclear. Using two well-established neurotoxic paradigms of MPTP-induced PD, involving an acute 7-day and a subacute 21-day regimen of MPTP, we showed that oral administration of TP-319 and TP-500 dose-dependently attenuated MPTP-induced loss of striatal DA and its metabolites and the loss of TH-immunopositive neurons in the substantia nigra. At doses as low as 0.5 μmol, both TP-319 and TP-500 showed comparable, but significantly higher level of potency than TP-224 in ameliorating MPTP-neurotoxicity. Despite all the three TP showing similar potency in dissociating the Nrf2/Keap1 complex in our Neh2-luc assay, the BBB permeability for TP-319 and TP-500 far exceeded that of TP-224, and therefore were more potent in inducing neuroprotective effects against MPTP neurotoxicity.

MPTP administration leads to marked increases in oxidative damage, activation of glia, and levels of proinflammatory cytokines, resulting in the initiation and/or perpetuation of nigrostriatal dopaminergic neurodegeneration. Postmortem human PD brains accumulate elevated levels of oxidative stress markers such as oxidized proteins, lipids, and nucleic acids (24), and abnormally activated glia that secrete toxic cytokines, chemokines, and complement proteins (2). Both TP-319 and TP-500 significantly blocked accumulation of the oxidative stress marker 3-nitrotyrosine, numbers of reactive microglia, in the substantia nigra, and increases in proinflammatory genes, suggesting that activation of the Nrf2 pathway by these TP is beneficial in blocking oxidative stress and neuroinflammation associated with MPTP neurotoxicity. In fact, multiple studies have convincingly demonstrated that CDDO and its synthetic analogs (methylamide, eythylamide, trifluoroethylamide, and methyl ester) block markers of oxidative stress and neuroinflammation in several models of neurodegenerative diseases (36, 41, 48).

The most striking and compelling evidence for activation of the Nrf2 pathway by TP-319 and TP-500 and its direct association in ameliorating MPTP neurotoxicity came from our studies using WT and Nrf2 KO mice. Both TP-319 and TP-500 significantly attenuated MPTP neurotoxicity in the WT mice, but not in the Nrf2 KO mice. These effects directly correlated with the ability of these TP to induce selective activation of Nrf2/ARE genes in the WT, but not in the Nrf2 KO mice. Among the prominent Nrf2-regulated genes induced by TP-319 and TP-500 in the nigrostriatal pathway were NQO1and HO-1 and genes involved in glutathione-dependent functions. In the context of PD, NQO1 induction may be important to nigrostriatal dopaminergic neurons due its relevance in the reduction of oxidized catechol rings and ameliorating the detrimental effects of DA quinones. NQO1 is also involved in detoxification of protein-bound quinones and maintains alpha-tocopherol and coenzyme Q_{10} in their reduced antioxidant states (44). Induction of HO-1 may provide resistance to chronic oxidative stress in dopaminergic neurons induced by the accumulation of iron due to its involvement in the metabolism of the pro-oxidant heme to the antioxidant pigment biliverdin (11). Genes involved in modulating GSH-dependent functions like glutamyl cysteine ligases and glutathione reductase are critical for dopaminergic neurons to detoxify xenobiotics by synthesis and conjugation of GSH to a range of electrophilic substrates. Importantly, maintenance of glutathione levels is also crucial for nigrostriatal dopaminergic neurons, since conditional knockdown of the catalytic subunit of glutamyl cysteine ligase in nigral dopaminergic neurons leads to a decline in GSH levels, and the progressive loss of

midbrain DA neurons in mice (5). Our studies conclusively demonstrate the remarkable ability of TP-319 and TP-500 to modulate crucial phase-2 antioxidant and cytoprotective genes that may be relevant for the survival of dopaminergic neurons in PD.

In summary, we have demonstrated that orally active, small-molecule synthetic TP such as TP-319 and TP-500 are extremely potent and direct activators of the Nrf2 pathway with robust neuroprotective properties in a toxin-induced preclinical model of PD. These results provide a strong rationale for further preclinical evaluation of such synthetic TP in more chronic models of PD harboring familial gene mutations. Collectively, these studies are expected to provide insights into how synthetic TP can be used most effectively for future clinical trials for the prevention and treatment of human PD.

Materials and Methods

Animals

Mice were housed and treated in strict accordance with the NIH Guide for the Care and Use of Laboratory Animals. All procedures were approved by the Institutional Animal Care and Use Committee of the Weill Medical College of Cornell University, New York. Mice were maintained in a pathogen-free facility and exposed to a 12-h light/dark cycle with food and water provided *ad libitum*. C57Bl6 mice were procured from Jackson laboratories, whereas Nrf2 KO mice used in the present study were on a pure C57Bl6 background (14). Age-matched WT and Nrf2 KO male mice used in the present study were obtained by crossing Nrf2 heterozygous mice.

N27 rat dopaminergic and human neuroblastoma SHSY5Y cell culture

Rat N27 cells were maintained in a medium containing RPMI 1640 (Invitrogen) with glutamine supplemented with 10% FBS, 100 U/ml penicillin, and 100 μg/ml streptomycin at 37°C in a humidified atmosphere of 5% CO_2. Cells were cultured up to 80% confluence in 12-well plates and treated with the respective doses of TP-319 and TP-500, indicated in the figure legends for real-time PCR, immunoblotting, and measurement of cellular GSH and GSSG levels. For nuclear translocation of Nrf2 from the cytosol, human neuroblastoma SHSY5Y cells were grown in the DMEM supplemented with high glucose and glutamine (Invitrogen) containing 10% FBS, 100 U/ml penicillin, and 100 μg/ml streptomycin. Cells were plated in 100-mm dishes, and when they were ~70% confluent, were treated with 100 n*M* of TP-319 or TP-500 for 0, 1, or 2 h. The NE-PER Nuclear and Cytosolic extraction kit (Thermo Scientific) was used to fractionate nuclear and cytosolic fractions according to the manufacturer's instruction.

Neh2-luc reporter assay

TP (30 n*M*–1 μ*M*) were tested in 96-well format white, flat-bottom plates in comparison with canonical Nrf2 activators TBHQ and sulforaphane (1–10 μ*M*). All stock solutions and their serial dilutions were prepared in DMSO. SHSY5Y cells expressing the Neh2-luc reporter (HIF1 ODD-luc reporter was used as a control line) were plated at the density of 30,000 cell per well using a WellMate multichannel dispenser from Matrix (Thermo Fisher Scientific) and grown overnight on DMEM/F12 + GlutaMAX (100 μl per well). Then, the compounds were added to each well, and the plates were incubated for a fixed time interval; the medium was removed; cells were lyzed; and luciferase activity was measured on a luminometer Lmax11384 (Molecular Devices) with BrightGlo™ reagent (Promega). The reporter activation was normalized to the background luminescence. Kinetics of reporter activation was measured by adding varied fixed concentrations of a studied compound at different time points followed by simultaneous cell lysis and activity measurement in the whole 96-well plate; this assay format minimizes experimental error originating from the well-known instability of the luciferase reagent. All experiments were performed in triplicate or quadruplicate.

Computer modeling

A 3D model of Keap1 was constructed using the crystal structure of FadR (PDB entry: 1e2x) as the template structure [as described in (47)]. Sequence alignment showed 14.6% and 36.3% of sequence identity and similarity, respectively. MODELER protocol (ver. 9v4) and Discovery Studio Software were used to generate 75 structural models of Keap1 IVR. The model with lowest objective function was selected for further study. Docking was performed by Discovery Studio Software using the LigandFit protocol with default parameters and CHARMm ligand minimization option. The ligand was treated as fully flexible, and the protein residues were kept restraint. Default scoring functions were enabled, and all poses were evaluated manually, and the best docking model was selected, respectively.

RNA isolation and real-time RT-PCR

Total RNA from N27 cells, mouse liver, striata, ventral midbrain, and cortex was isolated according to the manufacturer's protocol using TRIzol reagent (Invitrogen). About 2 μg of total RNA was reverse transcribed using a High-Capacity cDNA Reverse Transcription Kit (Invitrogen). cDNA was diluted, and 100 ng was used to amplify in an ABI prism 7900 HT Real-time PCR system (Applied Biosystems) for various genes using primers (Table 2) and Fast SYBR® Green Master Mix (Invitrogen). Cycling parameters were 95°C for 10 s, followed by 60°C for 1 min. Relative expression was calculated using the ΔΔCt method (25). Values are expressed as a fold of control reaction and normalized to glyceraldehyde-3-phosphate dehydrogenase (GAPDH) expression.

Western blot analysis

Protein extracts were prepared from N27 rat dopaminergic cells, human neuroblastoma SHSY5Y cells, mouse ventral midbrain, striata, and liver tissues by homogenization in a TNE buffer (10 m*M* Tris–HCl, pH 7.4, 150 m*M* NaCl, 5 m*M* EDTA, 0.5% NP-40, 1× Complete protease inhibitor cocktail [Roche], 1× phosphatase inhibitor cocktail I and II [Sigma]). Protein concentration was determined by BCA method (Pierce Biotech), and 25 μg of protein was resolved by sodium dodecyl sulphate–polyacrylamide gel electrophoresis (SDS-PAGE), transferred to nitrocellulose, and probed using appropriate primary antibodies (anti-Nrf2, [1:2000 Epitomics]; anti-Nrf2, [1:2000, C-20; Santa Cruz Biotechnology, Inc.]; anti-NQO1 [1:1000; Abcam], anti-glutathione reductase [1:2000; Abcam], anti- GCLC [1:10,000], anti-GCLM [1:10,000], anti-hemeoxygenase-1 [1:2500; Epitomics], anti-aldolase [1:1000;

Table 2. List of Primers and Their Sequences Used for Real-Time Polymerase Chain Reaction Studies

Gene	*Species*	*Accession*	*Left primer*	*Right primer*
Nrf2	Mouse	NM_010902.3	CATGATGGACTTGGAGTTGC	CCTCCAAAGGATGTCAATCAA
Nrf2	Rat	NM_031789.1	AGCATGATGGACTTGGAATTG	CCTCCAAAGGATGTCAATCAA
Gclm	Mouse	NM_008129.3	TGACTCACAATGACCCGAAA	GATGCTTTCTTGAAGAGCTTCCT
Gclm	Rat	NM_017305.2	CTGACTCACAATGACCCAAAAG	TTCAATGTCAGGGATGCTTTC
Gclc	Mouse	NM_010295.1	ATGATAGAACACGGGAGGAGAG	TGATCCTAAAGCGATTGTTCTTC
Gclc	Rat	NM_012815.2	GGCGATGTTCTTGAAACTCTG	CAGAGGGTTGGGTGGTTG
Nqo-1	Mouse	NM_008706.5	AGCGTTCGGTATTACGATCC	AGTACAATCAGGGCTCTTCTCG
Nqo-1	Rat	NM_017000.3	AGCGCTTGACACTACGATCC	CAATCAGGGCTCTTCTCACC
Ho-1	Mouse	NM_002133.2	GGGTGATAGAAGAGGCCAAGA	AGCTCCTGCAACTCCTCAAA
Ho-1	Rat	NM_012580.2	GTCAAGCACAGGGTGACAGA	CTGCAGCTCCTCAAACAGC
Gsr	Mouse	NM_010344.4	AGTTCCTCACGAGAGCCAGA	CAGCTGAAAGAAGCCATCACT
Gapdh	Mouse	NM_008084.2	GCCAAAAGGGTCATCATCTC	CACACCCATCACAAACATGG
Gapdh	Rat	NM_017008.3	TGGGAAGCTGGTCATCAAC	GCATCACCCCATTTGATGTT
Tnf	Mouse	NM_013693.2	TCTTCTCATTCCTGCTTGTGG	GGTCTGGGCCATAGAACTGA
Cd68	Mouse	NM_009853.1	GACCTACATCAGAGCCCGAGT	CGCCATGAATGTCCACTG
Ccl2	Mouse	NM_011333.3	CATCCACGTGTTGGCTCA	GATCATCTTGCTGGTGAATGAGT

Cd68, cluster of differentiation 68; *Gapdh*, glyceraldehyde-3-phosphate dehydrogenase; *Gclc*, glutathione cysteine ligase regulatory subunit; *Gclm*, glutathione cysteine ligase modulatory subunit; *Gsr*, glutathione reductase; *Ho-1*, hemeoxygenase 1; *Ccl2*, (*Mcp1*) monocyte chemotactic protein-1; *Nqo1*, NADPH quinone oxidoreductase 1; *Nrf2*, nuclear factor E2-related factor 2; *Tnf*, tumor necrosis factor.

Abcam], anti-PARP1 [1:1000; Santa Cruz Biotechnology, Inc.], and anti-GAPDH [1:5000; Fitzgerald]). Densitometric analyses were performed using Quantity One Software (Bio-Rad).

MPTP and triterpenoid administration in mice for neuroprotective studies

Acute and subacute MPTP intoxication paradigms were used to test the neuroprotective effects of TP using male C57Bl6 and/or Nrf2 KO and their age-matched WT littermates.

Acute MPTP. In this protocol, 10-week-old C57Bl6 mice ($n=8$ per group) were divided into four different groups consisting of (i) a control group treated with saline alone; (ii) a group treated with MPTP alone; (iii) a group treated with either TP-319 or TP-500 alone; and (iv) groups treated with TP-319 or TP-500 in combination with MPTP. TP-319 and TP-500 were dissolved in 1:4 ethanol:neobee oil (a derivative of coconut oil). MPTP 10 mg/kg free base was administered intraperitoneally three times a day every 2 h or at 15 mg/kg free base administered intraperitoneally four times a day every 2 h. Animals with TP-319 or TP-500 in combination with MPTP were administered TP by oral gavage with 4, 2, 1, and 0.5 μmol of the respective drugs in 100-μl volume once a day for 4 days before MPTP and once a day for 3 days after MPTP. On the day of MPTP, no drugs were administered to mice. Animals belonging to MPTP and control groups received the vehicle (ethanol:neobee oil, 1:4), whereas the drug-alone group received respective doses of triterpenoid drugs at the same frequency. All animals were sacrificed on the 7th day after MPTP. For neuroprotective studies in WT and Nrf2 KO mice, 10-week-old male Nrf2 KO and age-matched WT littermates were treated with 2 μmol of TP-319 or TP-500 at a similar frequency and volume described above. MPTP 10 mg/kg free base was administered four times a day every 2 h. All animals were sacrificed on the 7th day after MPTP.

Subacute MPTP. In this protocol, 12-week-old C57Bl6 mice ($n=8$ per group) were divided into the four different groups described above. MPTP 30 mg/kg free base was administered intraperitoneally once daily for 5 days. Animals with TP-319 or TP-500 in combination with MPTP were gavaged with 2 μmol of the respective triterpenoid in 100-μl volume once a day for 4 days before MPTP, again daily once 2 h before MPTP, and once a day for 3 days after MPTP. All animals were sacrificed 21 days after the last dose of MPTP.

Triterpenoid administration in mice for assessment of Nrf2-dependent genes

To test activation of the Nrf2/ARE pathway, *in vivo* male mice (C57Bl6 or Nrf2 KO and their age-matched WT littermates) were administered 4 μmol of TP (TP-319 or TP-500) in 100 μl of vehicle (ethanol:neobee oil, 1:4) by oral gavage twice 12 h apart. Control groups of mice received vehicle (ethanol: neobee oil, 1:4) at the same volume and frequency as TP. Mice were sacrificed, and the whole brain, striata, ventral midbrain, cortex, and liver were collected at 6, 9, 24, and 48 h after the last dose of each triterpenoid.

Measurement of tissue levels of TP by HPLC–mass spectrometry

Brain and liver (about 200–400 mg) tissue were homogenized on ice in 0.5 ml acetonitrile using Tissue Miser (Fisher Scientific). The homogenates were vortexed and then centrifuged at 21,000 *g*, at 4°C, for 10 min, and the supernatant was transferred and diluted 1:1 with 20 m*M* ammonium acetate pH 7.4. Diluted buffered acetonitrile extracts were centrifuged at 20,817 *g*, 4°C, for 5 min. Supernatants were loaded on a Waters XTerra MS C18 5-μm column, with initial column conditions 46% acetonitrile, 10 m*M* ammonium acetate, pH 7.4. The column was subjected to an 8-min gradient from 46% to 94% acetonitrile and then washed with 94% acetonitrile for 6 min. Compounds were detected using a Waters ZQ mass spectrometer with an electrospray ionization probe, positive ionization mode. Analysis was performed using the Waters MassLynx software package. Quantitation was against standard curves generated by adding dilutions of compounds to

the acetonitrile extract from control solid tissues and expressed as amount per wet weight of tissue (36).

Measurement of striatal levels of catecholamines and MPP^+ by HPLC

Striatal levels of DA and its metabolites DOPAC and HVA were measured after sonication and centrifugation in chilled 0.1 *M* perchloric acid (PCA, 100 μl/mg tissue) as previously described (48). Briefly, 15 μl supernatant was isocratically eluted through an 80-×4.6-mm C18 column (ESA, Inc.) with a mobile phase containing 0.1 *M* LiH_2PO_4, 0.85 m*M* 1-octanesulfonic acid, and 10% (v/v) methanol and detected by a 2-channel Coulochem II electrochemical detector (ESA, Inc.). Concentrations of DA, DOPAC, and HVA are expressed as ng per mg protein. The protein concentrations of tissue homogenates were measured according to the BCA assay (Pierce Biotech). For MPP^+ measurement, TP-319 or TP-500 was administered at a dose of 4 μmol once daily for 4 days followed by a dose on the 5th day, 30 min before MPTP. Striatal tissues were sonicated and centrifuged in 0.1 *M* PCA, and an aliquot of supernatant was injected onto a Brownlee aquapore×03-224 cation exchange column (Rainin). Samples were eluted isocratically with 20 m*M* boric acid–sodium borate buffer, pH 7.75, containing 3 m*M* tetrabutylammonium hydrogen sulfate, 0.25 m*M* 1-heptanesulfonic acid, and 10% isopropanol. MPP^+ levels were detected with a fluorescence detector set by excitation at 295 nm and emission at 375 nm (48).

Measurement of cellular GSH and GSSG levels by HPLC

N27 rat dopaminergic cells were sonicated in chilled 0.1 *M* PCA and centrifuged. Briefly, 15 μl supernatant was isocratically eluted through a 4.6-×150-mm C18 column (ESA, Inc.) with a mobile phase containing 50 m*M* LiH_2PO_4, 1.0 m*M* 1-octanesulfonic acid, and 1.5% (v/v) methanol and detected by a 2-channel Coulochem III electrochemical detector (ESA, Inc.), set with a guard cell potential 950 mV, Channel 1 potential for GSH detection and Channel 2 potential 880 mV for GSSG detection (48). Concentrations of GSH and GSSG are expressed as nmol per mg protein.

Immunohistochemistry and morphometric analysis

Mice were anesthetized with sodium pentobarbital, transcardially perfused with 0.9% saline, followed by 4% paraformaldehyde in 0.1 *M* phosphate-buffered saline (PBS), pH 7.4. Brains were dissected out, postfixed in 4% paraformaldehyde for 24 h, and cryopreserved in 30% sucrose/PBS for 48 h. Snap-frozen brains were coronally sectioned at 40-μm thickness, encompassing the substantia nigra using a cryostat. Briefly, sections were rinsed in PBS and incubated in 3% hydrogen peroxide/10% methanol solution for 10 min to quench endogenous peroxidase activity. Sections were permeabilized/blocked in 10% normal goat serum (NGS)/0.1% Triton X-100/PBS for 1 h at room temperature. Sections were incubated overnight at 4°C with the following primary antibodies in PBS containing 2% NGS/0.01% Triton X-100: rabbit polyclonal anti-TH (1:1000; Novus Biologicals), rat monoclonal anti-CD11b (1:500; Serotec), and rabbit polyclonal anti-3-nitrotyrosine (1:100; Calbiochem). Biotinylated secondary antibodies (Jackson ImmunoResearch Laboratories, Inc.) were used appropriately after incubation with streptavidin ABC solution (Vector Laboratories). Immunostaining was visualized by diaminobenzidine (Sigma) chromogen. Sections were mounted on glass, dehydrated, and cover-slipped with cytoseal (Thermo Scientific). Digital images were captured with a Coolpix 5000 Nikon Camera. TH-immunostained sections were counterstained with thionin before dehydration and cover-slipped with cytoseal. Nissl (thionin)-stained and TH-positive neuronal counts were estimated within the substantia nigra by Stereoinvestigator software (Microbrightfield) as previously described (39). CD11b-positive microglia were quantified on images captured from three coronal sections per mouse encompassing the substantia nigra. Quantitative analysis (cell number per square millimeter) was determined using NIH ImageJ software (50). SNpc 3-nitrotyrosine immunostaining was quantified by expressing the area occupied by the precipitate of 3-nitrotyrosine staining within the defined fields from three coronal sections per mouse encompassing the substantia nigra (45).

Statistical analysis

Results were expressed as means ± standard error of the mean. Significance was determined by one-way or two-way analysis of variance followed by the Student–Newman–Keuls test or a two-tailed unpaired Student *t*-test. Significance was set at $p \leq 0.05$. All statistical analyses were performed using Prism software (GraphPad).

Acknowledgments

This work was supported by grants from the NIH R21 NS062165 (BT), R01 NS060885 (BT), R01 ES017295 (MFB), R01 CA78814 (MBS), and Michael J. Fox Foundation for PD grant (BT and MFB), Department of Defense grant (MFB), Thomas Hartman Foundation for PD (IGG), Winifred Masterson Burke Relief Foundation (IGG), and Reata Pharmaceuticals Irving Texas. NAK is a PD Foundation postdoctoral fellow. We thank Dr. Terrance Kavanagh (University of Washington) for GCLC and GCLM antibodies and Dr. Curt Freed (University of Colorado) for rat dopaminergic $1RB_3AN_{27}$ (N27) cells.

Author Disclosure Statement

All authors declare no conflicts of interest.

References

1. Abiko Y, Miura T, Phuc BH, Shinkai Y, and Kumagai Y. Participation of covalent modification of Keap1 in the activation of Nrf2 by tert-butylbenzoquinone, an electrophilic metabolite of butylated hydroxyanisole. *Toxicol Appl Pharmacol* 255: 32–39, 2011.
2. Burguillos MA, Deierborg T, Kavanagh E, Persson A, Hajji N, Garcia-Quintanilla A, Cano J, Brundin P, Englund E, Venero JL, and Joseph B. Caspase signalling controls microglia activation and neurotoxicity. *Nature* 2011.
3. Burton NC, Kensler TW, and Guilarte TR. *In vivo* modulation of the Parkinsonian phenotype by Nrf2. *Neurotoxicology* 27: 1094–1100, 2006.
4. Chen PC, Vargas MR, Pani AK, Smeyne RJ, Johnson DA, Kan YW, and Johnson JA. Nrf2-mediated neuroprotection in the MPTP mouse model of Parkinson's disease: Critical role

for the astrocyte. *Proc Natl Acad Sci U S A* 106: 2933–2938, 2009.
5. Chinta SJ, Kumar MJ, Hsu M, Rajagopalan S, Kaur D, Rane A, Nicholls DG, Choi J, and Andersen JK. Inducible alterations of glutathione levels in adult dopaminergic midbrain neurons result in nigrostriatal degeneration. *J Neurosci* 27: 13997–14006, 2007.
6. Couch RD, Browning RG, Honda T, Gribble GW, Wright DL, Sporn MB, and Anderson AC. Studies on the reactivity of CDDO, a promising new chemopreventive and chemotherapeutic agent: implications for a molecular mechanism of action. *Bioorg Med Chem Lett* 15: 2215–2219, 2005.
7. Dexter DT, Sian J, Rose S, Hindmarsh JG, Mann VM, Cooper JM, Wells FR, Daniel SE, Lees AJ, Schapira AH, *et al.* Indices of oxidative stress and mitochondrial function in individuals with incidental Lewy body disease. *Ann Neurol* 35: 38–44, 1994.
8. Dinkova-Kostova AT, Liby KT, Stephenson KK, Holtzclaw WD, Gao X, Suh N, Williams C, Risingsong R, Honda T, Gribble GW, Sporn MB, and Talalay P. Extremely potent triterpenoid inducers of the phase 2 response: correlations of protection against oxidant and inflammatory stress. *Proc Natl Acad Sci U S A* 102: 4584–4589, 2005.
9. Dinkova-Kostova AT, Talalay P, Sharkey J, Zhang Y, Holtzclaw WD, Wang XJ, David E, Schiavoni KH, Finlayson S, Mierke DF, and Honda T. An exceptionally potent inducer of cytoprotective enzymes: elucidation of the structural features that determine inducer potency and reactivity with Keap1. *J Biol Chem* 285: 33747–33755, 2010.
10. Dumont M, Wille E, Calingasan NY, Tampellini D, Williams C, Gouras GK, Liby K, Sporn M, Nathan C, Flint Beal M, and Lin MT. Triterpenoid CDDO-methylamide improves memory and decreases amyloid plaques in a transgenic mouse model of Alzheimer's disease. *J Neurochem* 109: 502–512, 2009.
11. Ferris CD, Jaffrey SR, Sawa A, Takahashi M, Brady SD, Barrow RK, Tysoe SA, Wolosker H, Baranano DE, Dore S, Poss KD, and Snyder SH. Haem oxygenase-1 prevents cell death by regulating cellular iron. *Nat Cell Biol* 1: 152–157, 1999.
12. Fourquet S, Guerois R, Biard D, and Toledano MB. Activation of NRF2 by nitrosative agents and H2O2 involves KEAP1 disulfide formation. *J Biol Chem* 285: 8463–8471, 2011.
13. Huang HC, Nguyen T, and Pickett CB. Phosphorylation of Nrf2 at Ser-40 by protein kinase C regulates antioxidant response element-mediated transcription. *J Biol Chem* 277: 42769–42774, 2002.
14. Itoh K, Chiba T, Takahashi S, Ishii T, Igarashi K, Katoh Y, Oyake T, Hayashi N, Satoh K, Hatayama I, Yamamoto M, and Nabeshima Y. An Nrf2/small Maf heterodimer mediates the induction of phase II detoxifying enzyme genes through antioxidant response elements. *Biochem Biophys Res Commun* 236: 313–322, 1997.
15. Jakel RJ, Townsend JA, Kraft AD, and Johnson JA. Nrf2-mediated protection against 6-hydroxydopamine. *Brain Res* 1144: 192–201, 2007.
16. Jazwa A, Rojo AI, Innamorato NG, Hesse M, Fernandez-Ruiz J, and Cuadrado A. Pharmacological targeting of the transcription factor Nrf2 at the basal ganglia provides disease modifying therapy for experimental Parkinsonism. *Antioxid Redox Signal* 14: 2347–2360, 2011.
17. Jenner P. Oxidative stress in Parkinson's disease. *Ann Neurol* 53 Suppl 3: S26–S36; discussion S36–S28, 2003.
18. Kamat CD, Gadal S, Mhatre M, Williamson KS, Pye QN, and Hensley K. Antioxidants in central nervous system diseases: preclinical promise and translational challenges. *J Alzheimers Dis* 15: 473–493, 2008.
19. Kansanen E, Bonacci G, Schopfer FJ, Kuosmanen SM, Tong KI, Leinonen H, Woodcock SR, Yamamoto M, Carlberg C, Yla-Herttuala S, Freeman BA, and Levonen AL. Electrophilic nitro-fatty acids activate NRF2 by a KEAP1 cysteine 151-independent mechanism. *J Biol Chem* 286: 14019–14027, 2011.
20. Lee JM, Shih AY, Murphy TH, and Johnson JA. NF-E2-related factor-2 mediates neuroprotection against mitochondrial complex I inhibitors and increased concentrations of intracellular calcium in primary cortical neurons. *J Biol Chem* 278: 37948–37956, 2003.
21. Li J, Calkins MJ, Johnson DA, and Johnson JA. Role of Nrf2-dependent ARE-driven antioxidant pathway in neuroprotection. *Methods Mol Biol* 399: 67–78, 2007.
22. Liby K, Hock T, Yore MM, Suh N, Place AE, Risingsong R, Williams CR, Royce DB, Honda T, Honda Y, Gribble GW, Hill-Kapturczak N, Agarwal A, and Sporn MB. The synthetic triterpenoids, CDDO and CDDO-imidazolide, are potent inducers of heme oxygenase-1 and Nrf2/ARE signaling. *Cancer Res* 65: 4789–4798, 2005.
23. Liby KT, Yore MM, and Sporn MB. Triterpenoids and rexinoids as multifunctional agents for the prevention and treatment of cancer. *Nat Rev Cancer* 7: 357–369, 2007.
24. Lin MT and Beal MF. Mitochondrial dysfunction and oxidative stress in neurodegenerative diseases. *Nature* 443: 787–795, 2006.
25. Livak KJ and Schmittgen TD. Analysis of relative gene expression data using real-time quantitative PCR and the 2(-Delta Delta C(T)) Method. *Methods* 25: 402–408, 2001.
26. Moi P, Chan K, Asunis I, Cao A, and Kan YW. Isolation of NF-E2-related factor 2 (Nrf2), a NF-E2-like basic leucine zipper transcriptional activator that binds to the tandem NF-E2/AP1 repeat of the beta-globin locus control region. *Proc Natl Acad Sci U S A* 91: 9926–9930, 1994.
27. Neymotin A, Calingasan NY, Wille E, Naseri N, Petri S, Damiano M, Liby KT, Risingsong R, Sporn M, Beal MF, and Kiaei M. Neuroprotective effect of Nrf2/ARE Activators, CDDO-ethylamide and CDDO- trifluoroethylamide in a Mouse Model of Amyotrophic Lateral Sclerosis. *Free Radic Biol Med* 51: 88–96, 2011.
28. Niture SK, Jain AK, and Jaiswal AK. Antioxidant-induced modification of INrf2 cysteine 151 and PKC-delta-mediated phosphorylation of Nrf2 serine 40 are both required for stabilization and nuclear translocation of Nrf2 and increased drug resistance. *J Cell Sci* 122: 4452–4464, 2009.
29. Pacheco EA, Tiekink ERT, and Whitehouse MW. *Gold Chemistry: Applications and Future Directions in the Life Sciences,* edited by Fabian Mohr. Darmstadt, Germany: Wiley-VCH, 2009, p. 305.
30. Ramsey CP, Glass CA, Montgomery MB, Lindl KA, Ritson GP, Chia LA, Hamilton RL, Chu CT, and Jordan-Sciutto KL. Expression of Nrf2 in neurodegenerative diseases. *J Neuropathol Exp Neurol* 66: 75–85, 2007.
31. Rojo AI, Innamorato NG, Martin-Moreno AM, De Ceballos ML, Yamamoto M, and Cuadrado A. Nrf2 regulates microglial dynamics and neuroinflammation in experimental Parkinson's disease. *Glia* 58: 588–598, 2010.
32. Savitt JM, Dawson VL, and Dawson TM. Diagnosis and treatment of Parkinson disease: molecules to medicine. *J Clin Invest* 116: 1744–1754, 2006.
33. Schipper HM, Liberman A, and Stopa EG. Neural heme oxygenase-1 expression in idiopathic Parkinson's disease. *Exp Neurol* 150: 60–68, 1998.

34. Shen L and Ji HF. Insights into the disappointing clinical trials of antioxidants in neurodegenerative diseases. *J Alzheimers Dis* 19: 1141–1142, 2010.
35. Smirnova NA, Haskew-Layton RE, Basso M, Hushpulian DM, Payappilly JB, Speer RE, Ahn YH, Rakhman I, Cole PA, Pinto JT, Ratan RR, and Gazaryan IG. Development of Neh2-luciferase reporter and its application for high throughput screening and real-time monitoring of Nrf2 activators. *Chem Biol* 18: 752–765, 2011.
36. Stack C, Ho D, Wille E, Calingasan NY, Williams C, Liby K, Sporn M, Dumont M, and Beal MF. Triterpenoids CDDO-ethyl amide and CDDO-trifluoroethyl amide improve the behavioral phenotype and brain pathology in a transgenic mouse model of Huntington's disease. *Free Radic Biol Med* 49: 147–158, 2010.
37. Sykiotis GP and Bohmann D. Stress-activated cap'n'collar transcription factors in aging and human disease. *Sci Signal* 3: re3, 2010.
38. Thomas B, Banerjee R, Starkova NN, Zhang SF, Calingasan NY, Yang L, Wille E, Lorenzo BJ, Ho DJ, Beal MF, and Starkov A. Mitochondrial permeability transition pore component cyclophilin D distinguishes nigrostriatal dopaminergic death paradigms in the MPTP mouse model of Parkinson's disease. *Antioxid Redox Signal* 16: 855–868, 2012.
39. Thomas B, von Coelln R, Mandir AS, Trinkaus DB, Farah MH, Leong Lim K, Calingasan NY, Flint Beal M, Dawson VL, and Dawson TM. MPTP and DSP-4 susceptibility of substantia nigra and locus coeruleus catecholaminergic neurons in mice is independent of parkin activity. *Neurobiol Dis* 26: 312–322, 2007.
40. Thornalley PJ and Rabbani N. Dietary and synthetic activators of the antistress gene response in treatment of renal disease. *J Ren Nutr* 22: 195–202, 2012.
41. Tran TA, McCoy MK, Sporn MB, and Tansey MG. The synthetic triterpenoid CDDO-methyl ester modulates microglial activities, inhibits TNF production, and provides dopaminergic neuroprotection. *J Neuroinflammation* 5: 14, 2008.
42. Trinh K, Moore K, Wes PD, Muchowski PJ, Dey J, Andrews L, and Pallanck LJ. Induction of the phase II detoxification pathway suppresses neuron loss in Drosophila models of Parkinson's disease. *J Neurosci* 28: 465–472, 2008.
43. Tufekci KU, Civi Bayin E, Genc S, and Genc K. The Nrf2/ARE pathway: a promising target to counteract mitochondrial dysfunction in Parkinson's disease. *Parkinsons Dis* 2011: 314082, 2011.
44. van Muiswinkel FL and Kuiperij HB. The Nrf2-ARE Signalling pathway: promising drug target to combat oxidative stress in neurodegenerative disorders. *Curr Drug Targets CNS Neurol Disord* 4: 267–281, 2005.
45. Vereczki V, Martin E, Rosenthal RE, Hof PR, Hoffman GE, and Fiskum G. Normoxic resuscitation after cardiac arrest protects against hippocampal oxidative stress, metabolic dysfunction, and neuronal death. *J Cereb Blood Flow Metab* 26: 821–835, 2006.
46. von Otter M, Landgren S, Nilsson S, Celojevic D, Bergstrom P, Hakansson A, Nissbrandt H, Drozdzik M, Bialecka M, Kurzawski M, Blennow K, Nilsson M, Hammarsten O, and Zetterberg H. Association of Nrf2-encoding NFE2L2 haplotypes with Parkinson's disease. *BMC Med Genet* 11: 36, 2010.
47. Wu JH, Miao W, Hu LG, and Batist G. Identification and characterization of novel Nrf2 inducers designed to target the intervening region of Keap1. *Chem Biol Drug Des* 75: 475–480, 2010.
48. Yang L, Calingasan NY, Thomas B, Chaturvedi RK, Kiaei M, Wille EJ, Liby KT, Williams C, Royce D, Risingsong R, Musiek ES, Morrow JD, Sporn M, and Beal MF. Neuroprotective effects of the triterpenoid, CDDO methyl amide, a potent inducer of Nrf2-mediated transcription. *PLoS One* 4: e5757, 2009.
49. Yates MS, Tauchi M, Katsuoka F, Flanders KC, Liby KT, Honda T, Gribble GW, Johnson DA, Johnson JA, Burton NC, Guilarte TR, Yamamoto M, Sporn MB, and Kensler TW. Pharmacodynamic characterization of chemopreventive triterpenoids as exceptionally potent inducers of Nrf2-regulated genes. *Mol Cancer Ther* 6: 154–162, 2007.
50. Yin F, Dumont M, Banerjee R, Ma Y, Li H, Lin MT, Beal MF, Nathan C, Thomas B, and Ding A. Behavioral deficits and progressive neuropathology in progranulin-deficient mice: a mouse model of frontotemporal dementia. *FASEB J* 24: 4639–4647, 2010.
51. Yoo MS, Chun HS, Son JJ, DeGiorgio LA, Kim DJ, Peng C, and Son JH. Oxidative stress regulated genes in nigral dopaminergic neuronal cells: correlation with the known pathology in Parkinson's disease. *Brain Res Mol Brain Res* 110: 76–84, 2003.
52. Yore MM, Liby KT, Honda T, Gribble GW, and Sporn MB. The synthetic triterpenoid 1-[2-cyano-3,12-dioxooleana-1,9(11)-dien-28-oyl]imidazole blocks nuclear factor-kappaB activation through direct inhibition of IkappaB kinase beta. *Mol Cancer Ther* 5: 3232–3239, 2006.
53. Zhang Z, Chan GK, Li J, Fong WF, and Cheung HY. Molecular interaction between andrographolide and glutathione follows second order kinetics. *Chem Pharm Bull (Tokyo)* 56: 1229–1233, 2008.

Address correspondence to:
Dr. Bobby Thomas
Departments of Pharmacology & Toxicology and Neurology
Georgia Health Sciences University
1459 Laney Walker Blvd.
CB-3618
Augusta, GA 30912

E-mail: bthomas1@georgiahealth.edu

Date of first submission to ARS Central, December 21, 2011; date of final revised submission, June 25, 2012; date of acceptance, July 1, 2012.

Abbreviations Used

ARE = antioxidant response element
BBB = blood–brain barrier
Ccl2 = chemokine [C-C motif] ligand 2
CD68 = cluster of differentiation 68
CD11b = macrophage 1 antigen
CDDO = 2-cyano-3-,12-dioxooleana-1,9 (11)-dien-28-oic acid
DA = dopamine
DMSO = dimethylsulfoxide
DOPAC = 3,4-dihydroxyphenylacetic acid
GAPDH = glyceraldehyde-3-phosphate dehydrogenase
GCLC = glutathione cysteine ligase regulatory subunit

Abbreviations Used (Cont.)

GCLM = glutathione cysteine ligase modulatory subunit
GSH = reduced glutathione
Gsr = glutathione reductase
GSSG = oxidized glutathione
HIF = hypoxia inducible factor
HO-1 = hemeoxygenase 1
HPLC = high-performance liquid chromatography
HVA = homovanillic acid
IVR = intervening region
Keap1 = Kelch-like ECH-associated protein 1
KO = knockout
MCP-1 = monocyte chemotactic protein-1
MPP^+ = 1-methyl-4-phenyl-pyridinium ion
MPTP = 1-methyl-4-phenyl-1,2,3,6-tetra-hydropyridine
mRNA = messenger RNA
NGS = normal goat serum
NQO1 = NADPH quinone oxidoreductase 1
Nrf2 = nuclear factor E2-related factor 2
PARP1 = poly-ADP ribose polymerase 1
PBS = phosphate-buffered saline
PCA = perchloric acid
PD = Parkinson's disease
RT-PCR = reverse transcriptase–polymerase chain reaction
SDS-PAGE = sodium dodecyl sulphate–polyacrylamide gel electrophoresis
SNpc = substantia nigra pars compacta
TBHQ = tert-butylhydroquinone
TNF-α = tumor necrosis factor-alpha
TH = tyrosine hydroxylase
TP = triterpenoids
WT = wild-type